geologica acta

Citation: Torromé, D., Martín-Pérez, A., Košir, A., Aurell, M., 2024. Controls on carbonate deposition and microbialite formation in distal alluvial systems (Campanian, Montalbán subbasin, NE Spain). Geologica Acta, 22.12, 1-pgs.

Online ISSN: 1696-5728 DOI: 10.1344/GeologicaActa2024.22.12

Controls on carbonate deposition and microbialite formation in distal alluvial systems (Campanian, Montalbán subbasin, NE Spain)

Diego Torromé[1] **Andrea Martín-Pérez**[2, 3] **Adrijan Košir**[2] **Marcos Aurell**[1]

[1]Earth Sciences Department-IUCA, University of Zaragoza
C. de Menéndez Pelayo, 24, 50009, Zaragoza, Spain. Torromé E-mail: dtorrome@gmail.com; Aurell E-mail: maurell@unizar.es

[2]Ivan Rakovec Institute of Palaeontology, Research Centre of the Slovenian Academy of Sciences and Arts
Novi trg 2, 1000, Ljubljana, Slovenia. Martín-Pérez E-mail: andreamp@zrc-sazu.si; Košir E-mail: adrijan@zrc-sazu.si

[3]Postgraduate School ZRC SAZU
Ljubljana, Slovenia

ABSTRACT

The middle-upper Campanian Allueva Formation was deposited in the compressional intramountain Montalbán subbasin (central Iberian Ranges, NE Spain). This *i.e.* formation consists of alluvial terrigenous deposits, with local dominance of carbonates and microbialites, which are the main focus of this study. Three sfacies associations are differentiated: i) bioclastic facies association including limestone levels with accumulation of gastropods and charophytes, along with polygenetic carbonate breccias; ii) microbialite facies association dominated by irregular limestone beds rich in oncoids; iii) terrigenous facies association including metric levels of reddish-brown mudstone with intercalations of sandstones and conglomerates. These facies deposited in a low water level and short residence lacustrine-palustrine environments, in the distal areas of an alluvial system. Isotopic data ($\delta^{13}C$ and $\delta^{18}O$) fall in the range of freshwater carbonates and support this interpretation. The most common microbialites are oncoids, which have been classified into six types based on their morphology, size, and lamination. Cyclic patterns in the lamination of oncoids have been related to changing wet and dry conditions. Our results suggest that the alluvial setting was mainly fed by meteoric waters, with a sub-humid climate gradually transitioning to more arid conditions.

KEYWORDS | **Microbialites. Oncoids. Cretaceous. Iberia. Alluvial.**

INTRODUCTION

Lacustrine settings with microbialites form under the influence of a combination of tectonic, climatic, and hydrological conditions (Shapiro *et al.*, 2009; Arenas-Abad *et al.*, 2010; Bosence, 2012). Understanding the processes controlling the genesis of microbialites provides key information for the paleoenvironmental interpretation (Andres and Reid, 2006). The significance of microbialites in marine settings has been extensively studied (*e.g.* Jahnert and Collins, 2011, 2013; Mercedes-Martín *et al.*, 2014; Sequero *et al.*, 2020). However, the relationship between

microbialites, their genesis (Andres and Reid, 2006; Cloud, 1942), and their facies associations in lacustrine settings remains a topic of ongoing debate (*e.g.* Martín-Bello *et al.*, 2019; Noffke and Awramik, 2013; Renaut *et al.*, 2013; Roche *et al.*, 2018). Furthermore, oncoids, the main type of microbialite studied in this work, are significantly less documented than stromatolites in the scientific literature.

In the Iberian Peninsula, the pioneering studies by Ordóñez and García del Cura (1977, 1983) in the Cenozoic Duero Basin described discontinuous oncolite levels associated to lacustrine facies, as well as tufa-like deposits in Neogene fluvial carbonates of Central Spain. Similar settings in Iberia include the alluvial fans of the Upper Oligocene Montgat area (Catalan Coastal Ranges), where up to 20cm-diametre oncoids are found in pond deposits (Parcerisa *et al.*, 2006). Monty and Mas (1981) described different facies associations containing microbialites in a marginal-marine environment from the Lower Cretaceous of the Levantine Sector of the Iberian Ranges. In the South-Central Pyrenees, the widespread occurrence of Upper Cretaceous lacustrine oncolites was linked to a period of ecological crisis (Astibia *et al.*, 2012; Freeman *et al.*, 1982). Also relevant is the study of the Lower Cretaceous fluvial oncoids of the Cedar Mountain Formation (Fm.) in Utah (Shapiro *et al.*, 2009), which show significant similarities to these in the present study, like the local presence of dinosaur bones in the oncoid nuclei.

The carbonate succession with microbialites studied here belongs to the Allueva Fm., a middle-upper Campanian (uppermost Cretaceous) alluvial unit deposited during the initial stages of development of the intramountain Montalbán subbasin (central Iberian Ranges). Aurell *et al.* (2022) described the overall stratigraphy and sedimentology of the Allueva Fm., while Torromé and Aurell (2024) provided a preliminary description of the continental oncoids found in this unit. However, a detailed analysis of the microbialites, nor an examination of their facies associations and lateral relationships has not been yet performed. Consequently, the present study aims to: i) provide a detailed description of facies and their lateral and vertical distribution; ii) describe, analyse and interpret the different types of microbialites found in the Allueva Fm.; iii) establish a paleoenvironmental interpretation; iv) provide new insights on the climatic and hydrological controls of the system and v) extend the Cretaceous lacustrine oncoids record by comparing the findings with other microbialite deposits under similar conditions, particularly those associated with vertebrate assemblages.

GEOLOGICAL SETTING

The Iberian Basin rift system was formed due to the tectonic extension that dominated most of the Mesozoic in northeast Iberia (*e.g.* Salas and Casas, 1993). The onset of the NW-SE trending Iberian Basin rift system occurred during the Late Permian-Early Triassic rifting phase (Sánchez-Moya and Sopeña, 2004). Following the development of extensive shallow-marine carbonate platforms during most of the Jurassic, a second rifting episode in the latest Jurassic to Early Cretaceous led to the formation of various independent sedimentary basins within the system (Salas *et al.*, 2001; Aurell *et al.*, 2019; Martín-Chivelet *et al.*, 2019). During the Late Cretaceous post-rift phase, extensive carbonate platforms developed in the Iberian Seaway, a large subsiding area located between the emerged Iberian and Ebro massifs (*e.g.* Floquet, 1991). Towards the end of the Cretaceous, a progressively marine regressive trend was recorded in all domains of the Iberian Basin (García *et al.*, 2004; Segura *et al.*, 2004; Martín-Chivelet *et al.*, 2019). In the Maestrazgo domain, located in the southeastern Iberian Basin (Fig. 1A), this regressive trend is reflected in the transition from the coastal limestones and marlstones of La Cañadilla Fm. (upper Santonian-lower Campanian; Torromé *et al.*, 2022), to the palustrine-lacustrine limestones of the Fortanete Fm. (lower Campanian; Torromé *et al.*, 2023).

The tectonic inversion of the Iberian Basin rift system during the Alpine compression gave rise to the Iberian Ranges. Although the main phase of the Alpine orogeny took place during the Eocene-early Miocene (*e.g.* Casas *et al.*, 2000; Liesa *et al.*, 2018), the initial stages of inversion of the rift system began in the latest Cretaceous, from the middle Campanian onwards (Aurell *et al.*, 2022; Martín-Chivelet *et al.*, 2019). In the Maestrazgo domain, the middle-upper Campanian alluvial Allueva Fm. was deposited contemporaneously with the initial stages of uplift of the southern flank of the Montalbán anticline (Aurell *et al.*, 2022), a large Alpine compressional structure located in the northeastern Iberian Range.

The Montalbán subbasin corresponds to a 50km length intramountain syncline structure bounded to the south by the Utrillas thrust and to the north by the Montalbán anticline (Fig. 1A). The Allueva Fm. consists of an terrigenous-dominated alluvial succession up to 700m-thick (Fig. 1B), subdivided into 4 subunits (A1 to A4; Aurell *et al.*, 2022; Fig. 1B). Subunits A1, A3 and A4 are dominated by terrigenous deposits, mostly m-thick reddish-brown mudstones with interbedded sandstones (laminated or burrowed) and conglomerates. Subunit A2 studied here is locally dominated by continental carbonates, which contain abundant fossils (dinosaur bones, eggshells, gastropods, charophytes and microbialite structures).

METHODOLOGY

A bed-by-bed analysis of the subunit A2 was performed across four stratigraphic logs, distributed over a 10km

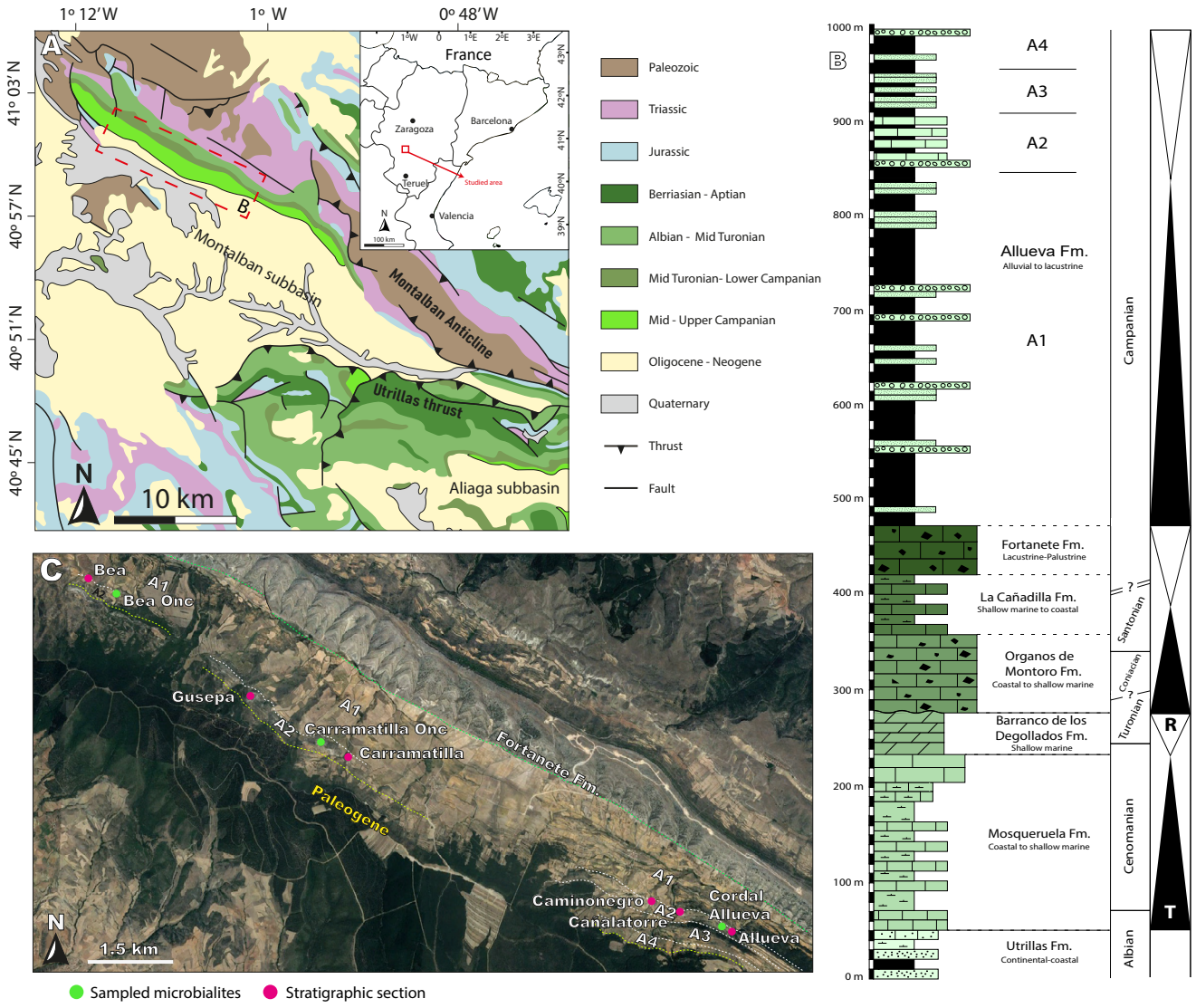

FIGURE 1. A) Geological map of the study area. B) Synthetic stratigraphic log of the uppermost Cretaceous in the Maestrazgo domain. C) Aerial image of the study area, showing the boundaries of geological formations and subunits of the Allueva Fm. Red circles indicate stratigraphic logs, while green circles mark additional sites rich in microbialites (compiled from Aurell *et al.*, 2022 and Torromé *et al.*, 2022, 2023).

section in the northwestern marginal areas of the Montalbán subbasin (see Fig. 1C for location). The thickness of the unit ranges from 66m in the Gusepa section, to 48m in the Carramatilla section. Facies descriptions are based on field observations and the analysis of 31 polished slabs and 37 thin sections. The $CaCO_3$ content was determined in 14 marlstone samples using calcimetry. Marlstones were also sieved to identify possible fossil assemblages, including vertebrate remains (eggshells, teeth).

The textural description follows the classification by Dunham (1962). Several features of lacustrine/palustrine environments are described based on the definitions of Freytet and Plaziat (1982) and Alonso-Zarza and Wright (2010), while the description of microbialites is mainly based on the classifications and descriptions of Logan *et al.* (1964), Monty (1976), Kennard and Burne (1989) and Riding (1991, 2000, 2008, 2011). Following Flügel (2004), the term 'oncoid' refers to individual grains, while 'oncolite' is used to describe a rock composed of numerous oncoids.

Selected thin sections and slabs were analysed at the Institute of Palaeontology ZRC SAZU (Ljubljana, Slovenia) using a JEOL JSM-IT100 Scanning Electron Microscope (SEM) with an Energy Dispersive X-ray Spectroscopy detector (EDS). Thin sections were mounted with carbon tape onto aluminium stubs and examined at an accelerating voltage of 15kV and working distance of 10mm. Uncoated samples were analysed under low vacuum (40Pa), while carbon-coated samples

were observed under high vacuum. Pictures were taken in Backscattered Electron mode (BES). Qualitative and semi-quantitative elemental analyses (EDS) were performed in low and high-vacuum conditions.

Cathodoluminescence imaging of polished thin sections was carried out at the Karst Research Institute ZRC SAZU, Postojna, Slovenia, using a Technosyn cold CL luminoscope (model CITL CL8200 MK4) with a 14-15kV electron beam energy and an electron current of 350-400μA, mounted on a Nikon Eclipse E600 petrographic microscope. Cathodoluminescence images were taken with an Olympus SC180 digital camera connected to a computer with a cellSens Entry imaging software package.

A $\delta^{13}C$ and $\delta^{18}O$ isotopic analysis was performed on 14 samples taken from the Carramatilla section. The analysis was conducted on the remaining slabs from thin sections to observe under the petrographic microscope any diagenetic feature that could alter the primary isotopic signal. Sample powder (>0.1g) was obtained by crushing the rocks with a pestle and sieving to 53 μm, then stored in Eppendorf tubes. To determine the isotopic relations $\delta^{13}C/\ \delta^{12}C$ and $\delta^{18}O/\ \delta^{16}O$, CO_2 was extracted by reaction with H_3PO_4 (103% and 90ºC) using the ISOCARB system. CO_2 was analysed by mass spectrometry (SIRA-II model) in Dual Inlet mode. This analysis was performed in the "Servicio de análisis de isótopos estables" at the University of Salamanca (Spain).

FACIES ANALYSIS

The distal alluvial succession of the Allueva Fm. studied here (subunit A2) includes eight sedimentary facies (Fig. 2), which are grouped into three facies associations: B for bioclastic, M for microbialites, and T for terrigenous facies. Figure 3 shows the lateral and vertical distribution of these facies, based on the correlation of the stratigraphic logs of Gusepa, Carramatilla, Caminonegro, and Cañalatorre. The logs from Bea and Allueva (taken from Aurell *et al.*, 2022) are also included to highlight the lateral boundaries of the studied lacustrine/palustrine sector.

Bioclastic facies association

The bioclastic facies association includes limestones and marlstones, with frequent intercalations of red beds (Fig. 4A). Three facies (B1 to B3) were characterized based on different proportions of skeletal (mainly gastropods and charophytes) and non-skeletal grains (mainly intraclasts and calcareous nodules).

Facies B1 consists of grey to dark-grey weakly bioturbated dm- to up to 4m-thick marlstone beds. The $CaCO_3$ content ranges between 40 and 60%. Fossil content is variable, with the common presence of gastropod fragments (<1cm). Some levels are rich in charophytes (*Microchara*, *Bysmochara, Strobilochara, Nitellopsis*, and *Lychnothamnus*; Aurell *et al.*, 2022), eggshell

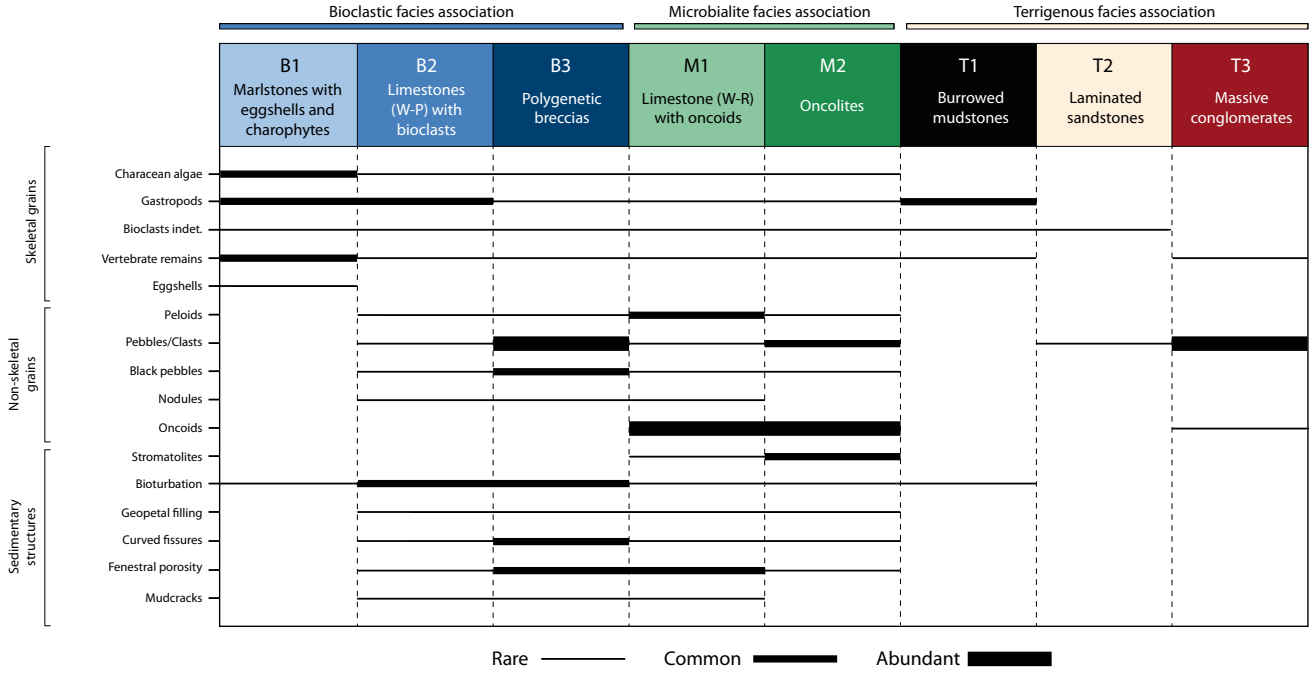

FIGURE 2. Relative abundance of skeletal and non-skeletal components, and main sedimentary structures observed in the eight facies identified in the A2 subunit (upper Allueva Fm.).

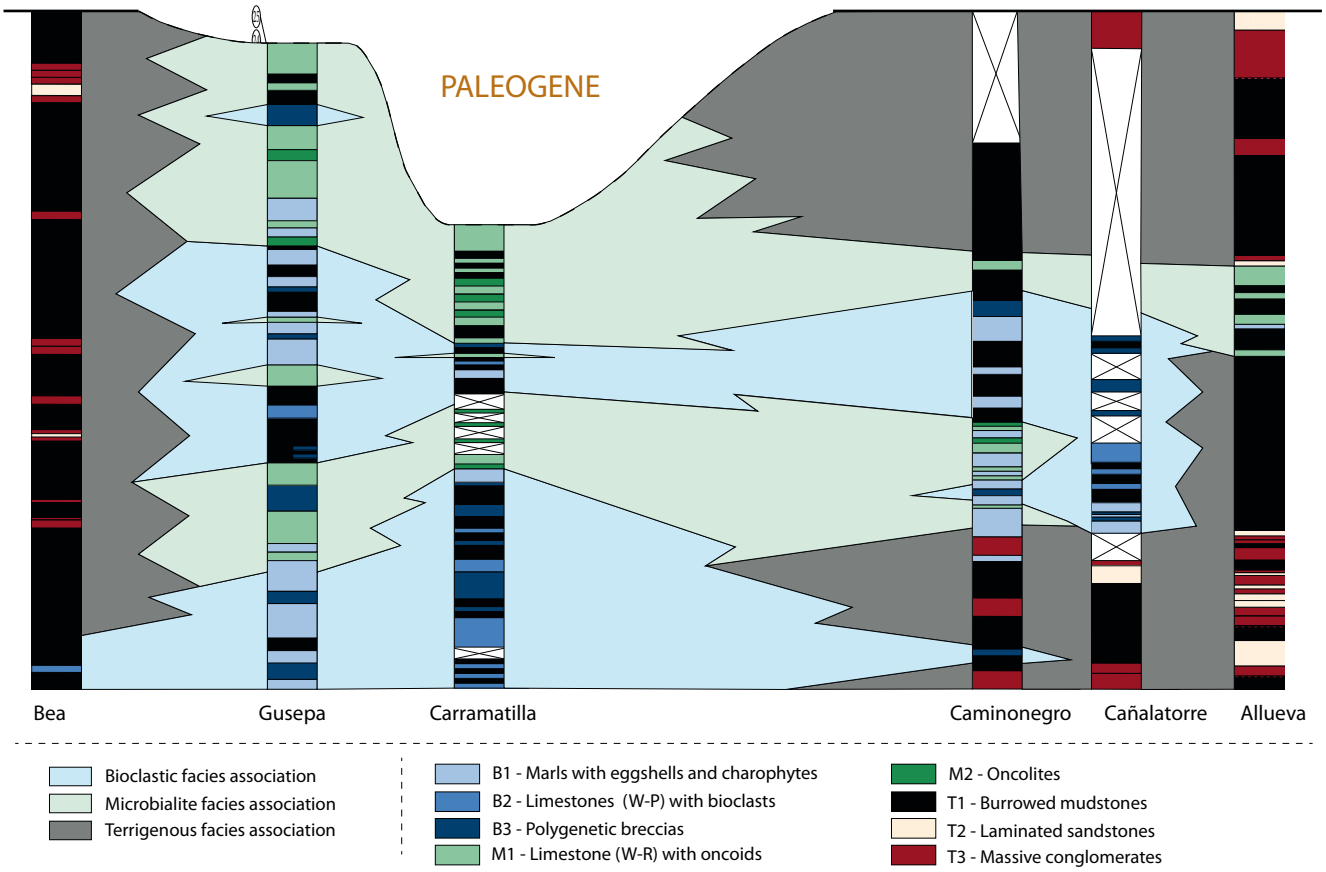

FIGURE 3. Overall distribution of facies associations in the A2 subunit (Allueva Fm.) between Bea and Allueva (see Fig. 1C for location).

fragments (*Pseudogeckoolithus*; Choi *et al.*, 2018) and vertebrate remains (Fig. 4B).

Facies B2 consists of grey bioclastic wackestone to packstone beds ranging from decimeters to meters in thickness (up to 6m). Identified fossils include gastropods, rare charophytes (Fig. 4C-D) and isolated vertebrate remains. Small and rounded mm-sized intraclasts are common (Fig. 4D). Frequent vertical traces are associated with microstructures such as geopetal infillings of fenestral pores and circumgranular fissures (Fig. 4D).

Facies B3 consists of dm- to up to 5m-thick tabular beds dominated by clasts of diverse origin, size, composition and roundness, giving rise to polygenetic breccias (Fig. 4E). The clasts range from mm- to cm-sized (usually <5cm). Black pebbles are common, along with calcareous nodules (Fig. 4F). In the northwestern log of Gusepa, the matrix includes lens-shaped gypsum crystals (Fig. 4F). Vertical traces and sparite-filled fenestral pores are common, along with curved (circumgranular) fissures surrounding clasts and nodules. Vertebrate remains are very rare.

Microbialite facies association

The microbialite facies association comprises two limestone facies (M1 and M2; Fig. 2), characterized by the presence of oncoids. These limestones are locally channelized and show significant lateral thickness variation (Fig. 5A).

Facies M1 occurs in dm- to m-thick (up to 4m) tabular to lenticular levels of grey limestones with lateral variation of facies. The dominant wackestone to rudstone textures, characterized by mm- to cm-sized coated grains (small oncoids), result in a tufa-like deposit (Fig. 5B-C). Coated grains are usually elongated, while spherical shapes are less common. Fossil content is scarce (fragmented gastropods and charophytes), which may also present coatings. Sparite-filled fenestral pores are common. Peloids, intraclasts, and stromatactis-like structures (Fig. 5D) (Deelman, 1972) are less abundant. The fillings of the stromatactis-like cavities include three different phases of cementation: the first phase (CC1) consists of silt-size carbonate sediment, forming geopetal infillings; the second phase (CC2) involves equant calcite crystals lining the pore walls; and a third phase (CC3) comprises larger crystals giving rise to

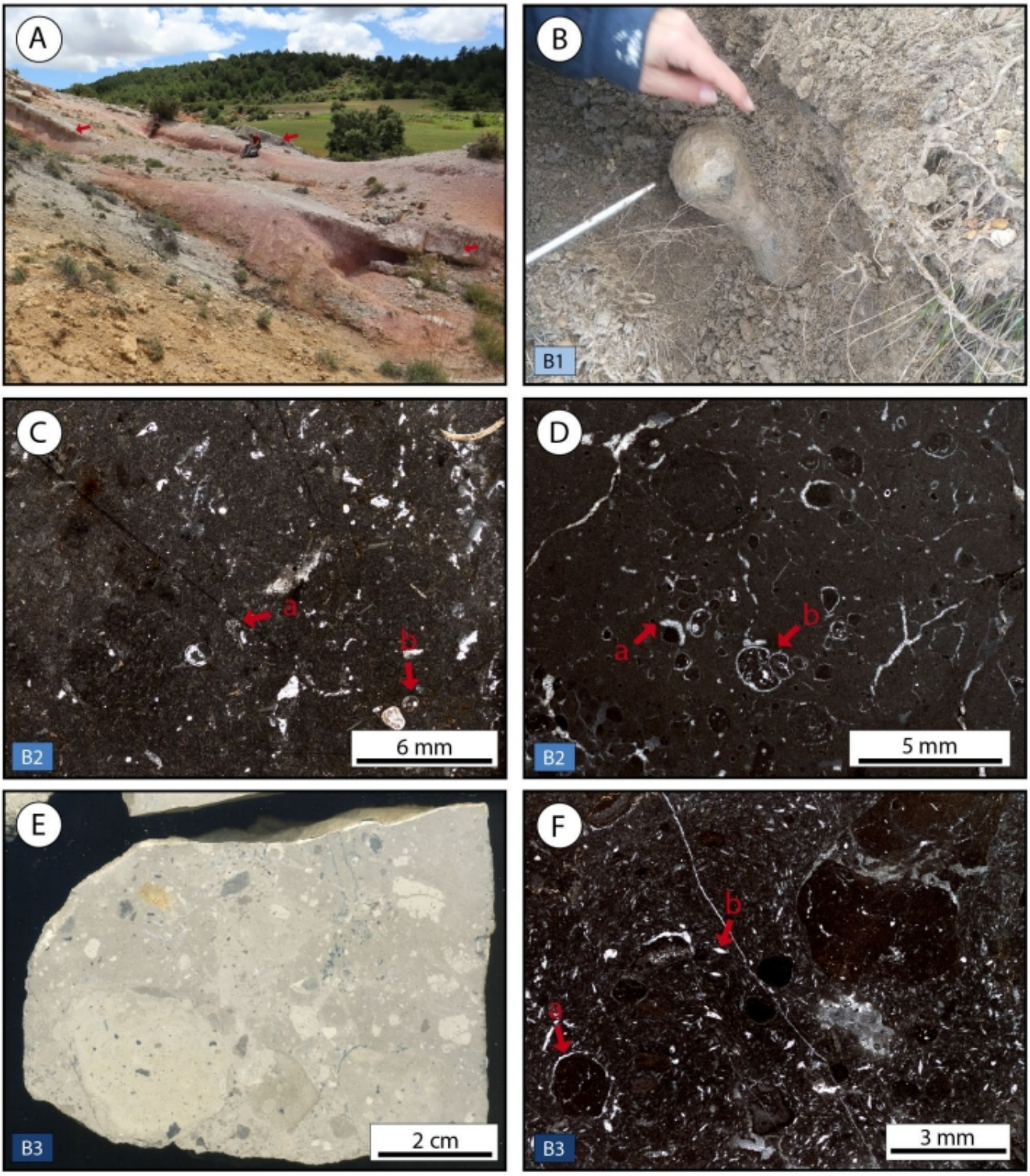

FIGURE 4. A) View of the Cañalatorre section showing intercalations of m-thick red mudstones, grey marlstones and dm-thick levels of white limestones (red arrows). B) Facies B1: dark-grey marlstone with a dinosaur vertebra. C) Facies B2: wackestone with fragmented gastropods (b) and isolated charophyte debris (a). D) Facies B2: wackestone containing small black pebbles with circumgranular cracks (a) and gastropods (b). E) Facies B3: polygenetic breccia with pebbles of different colours and degrees of roundness. F) Facies B3: polygenetic breccia featuring well-rounded black pebbles showing circumgranular cracks (a) and gypsum crystals (b), along with desiccation fractures and gastropods.

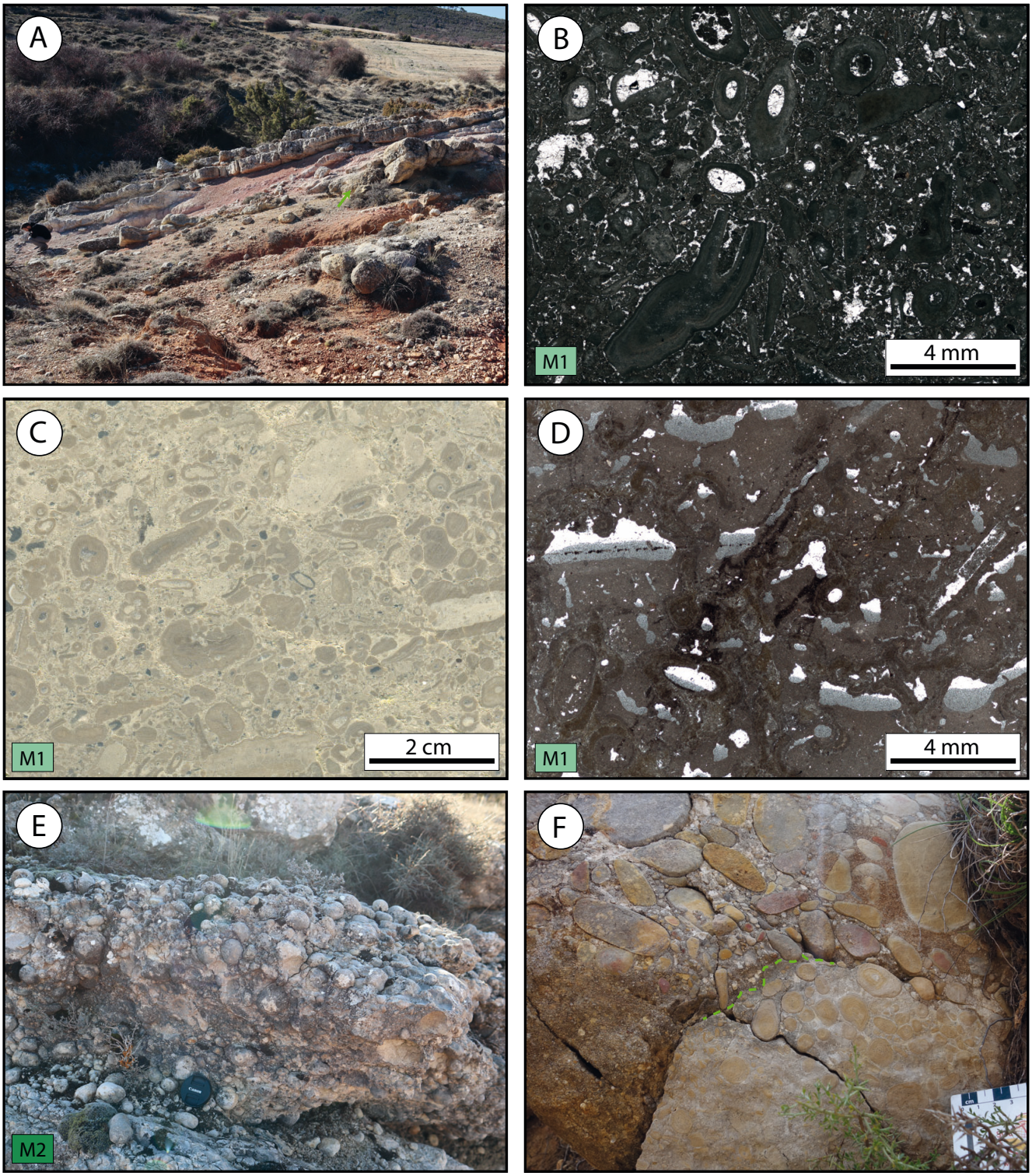

FIGURE 5. A) View of the Carramatilla section showing intercalations of m-thick reddish-brown mudstones with grey limestones. Arrow points to a channelized oncolite bed. B) Facies M1: rudstone with small mm-sized oncoids and coated grains. C) Facies M1: rudstone with small-sized oncoids and coated grains. D) Facies M1: stromatactis-like pores showing geopetal fillings. The surrounding matrix show diverse coated grains and small-sized oncoids. E) Facies M2: oncolite composed of oncoids of various sizes, lens cap is 7.5cm. F) Sharp contact between conglomerates and oncolites represented as an erosive surface, indicated by a green dashed line.

a blocky cement (Fig. 6A-E). Under cathodoluminescence, CC2 cements display a well-defined internal zonation, alternating between bright yellow-orange luminescence layers and non-luminescent zones, whereas CC3 displays dull luminescence (Fig. 6F).

Facies M2 is characterized by grey oncolitic lenticular beds, ranging from several dm to 1m in thickness. Pseudo-spherical oncoids commonly occur in poorly sorted accumulations (Fig. 5E). These can form isolated beds or appear at the top of beds dominated by facies M1, with an upwards size increase. The size of oncoids is variable, ranging in diameter from 5cm to more than 10cm. Lateral extension of these beds is limited due to their lenticular shape and the presence of erosive channels (Fig. 5F). Desiccation-related structures, such as fenestral porosity and circumgranular fissures, are locally present. Isolated bones (*e.g.* titanosaur caudal vertebrae) are also found, some of which show microbial carbonate coatings.

Terrigenous facies association

This facies association includes alternating mudstones, sandstones and conglomerates (Fig. 7A), which correspond to the facies T1, T2 and T3, respectively (Fig. 2). These terrigenous facies represent the lateral equivalents of the carbonate dominated facies associations described above (Fig. 3).

Facies T1 consists of m-thick reddish-brown bioturbated mudstones with scattered, cm-sized rounded pebbles. Fossil content includes small gastropods, while vertebrate remains are scarce but well-preserved (Fig. 7B).

Facies T2 is dominated by dm- to m-thick reddish-brown cross-bedded sandstones (Fig. 7C), which grade laterally into burrowed massive sandstones. Grain-size is variable, with occasional small, mm-sized soft pebbles.

Facies T3 forms conglomerate beds 1 to 5m-thick, often exhibiting channel geometries and occasional cross-bedding. The conglomerates are grain-supported and dominated by cm-size sub-rounded carbonate pebbles (Fig. 7D). The size of the pebbles varies from several millimetres to over 10cm. Isolated vertebrate remains and oncoids are locally present.

Facies and paleoenvironmental interpretation

The Allueva Fm. was deposited in the middle and distal areas of a complex alluvial system (Aurell *et al.*, 2022; Fig. 8A). Dispersed lakes developed in the distal alluvial setting, adjacent to active channels (Fig. 8B). Coarse-grained layers were associated with a braided channel system, characterized by high lateral variability (Pérez *et al.*, 1983). Massive conglomerates correspond to the bar nuclei, whereas cross-bedded intervals are related to lateral and frontal bar migration (Allen, 1983; Huerta *et al.*, 2011; McGowan and Groat, 1971). In addition, lenticular and massive conglomerate beds with incised erosive surfaces and lower sorting/roundness are probably related to episodic high-energy events, such as flash floods (*e.g.* Long, 2017; Sohn *et al.*, 1999). The fine-grained reddish-brown mudstones represent floodplains, oxidized under subaerial exposure conditions, while intercalated dark-grey mudstones indicate more humid floodplain areas with ponding. These areas were probably submerged only during periods of high discharge, which facilitated the colonization of invertebrate fauna (Miall, 1977; Nichols and Fisher, 2007).

The bioclastic and microbialite facies associations were deposited in ephemeral lacustrine to palustrine environments (Fig. 8B). Evidence of desiccation (spar-filled mudcracks, stromatactis-like fenestral pores, and circumgranular cracks), suggests fluctuating water levels. Desiccation plays a key role at lake margins, promoting brecciation, often in combination with root bioturbation (Freytet and Plaziat, 1982).

Charophytes, like other rooted aquatic plants, are common colonizers of lake margins (*e.g.* Alonso-Zarza and Wright, 2010; Platt and Wright, 1991). The accumulation of charophytes and gastropods in facies B1 and B2 likely occurred far from the channel-lake interface, where energy levels were lower, and water levels remained more stable over time. The widespread lacustrine association of gastropods and charophytes is well documented in the Cretaceous of the Iberian Peninsula (*e.g.* Freeman *et al.*, 1982; Martín-Chivelet and Gimenez, 1992; Monty and Mas, 1981; Torromé *et al.*, 2023; Vicente *et al.*, 2016). However, the scarcity of marlstone beds with a high proportion of charophytes suggests that turbulence and detrital input were too high for their full proliferation (*e.g.* García and Chivas, 2006). Microbialites develop along lake shorelines and in shallow waters, both as oncoids and stromatolites (*e.g.* Parcerisa *et al.*, 2006). Vertical traces related to root bioturbation are less common in beds containing microbialites.

Tufa-like accumulations of small coated grains have been described in isolated ephemeral ponds, in lakes during periods of low water levels, or in low-sinuosity, slow-flowing channels (*e.g.* Alonso-Zarza and Calvo, 2000; Alonso-Zarza and Wright, 2010; Arenas *et al.*, 2007; Vázquez-Urbez *et al.*, 2013; Zamarreño *et al.*, 1997). Lenticular beds of facies M1 lack sharp erosive surfaces and may be associated with slow-flowing channels, whereas tabular layers with greater lateral continuity are likely linked to ephemeral ponds. Oncoids usually require higher-energy conditions and turbulence to form (Logan *et al.*, 1964).

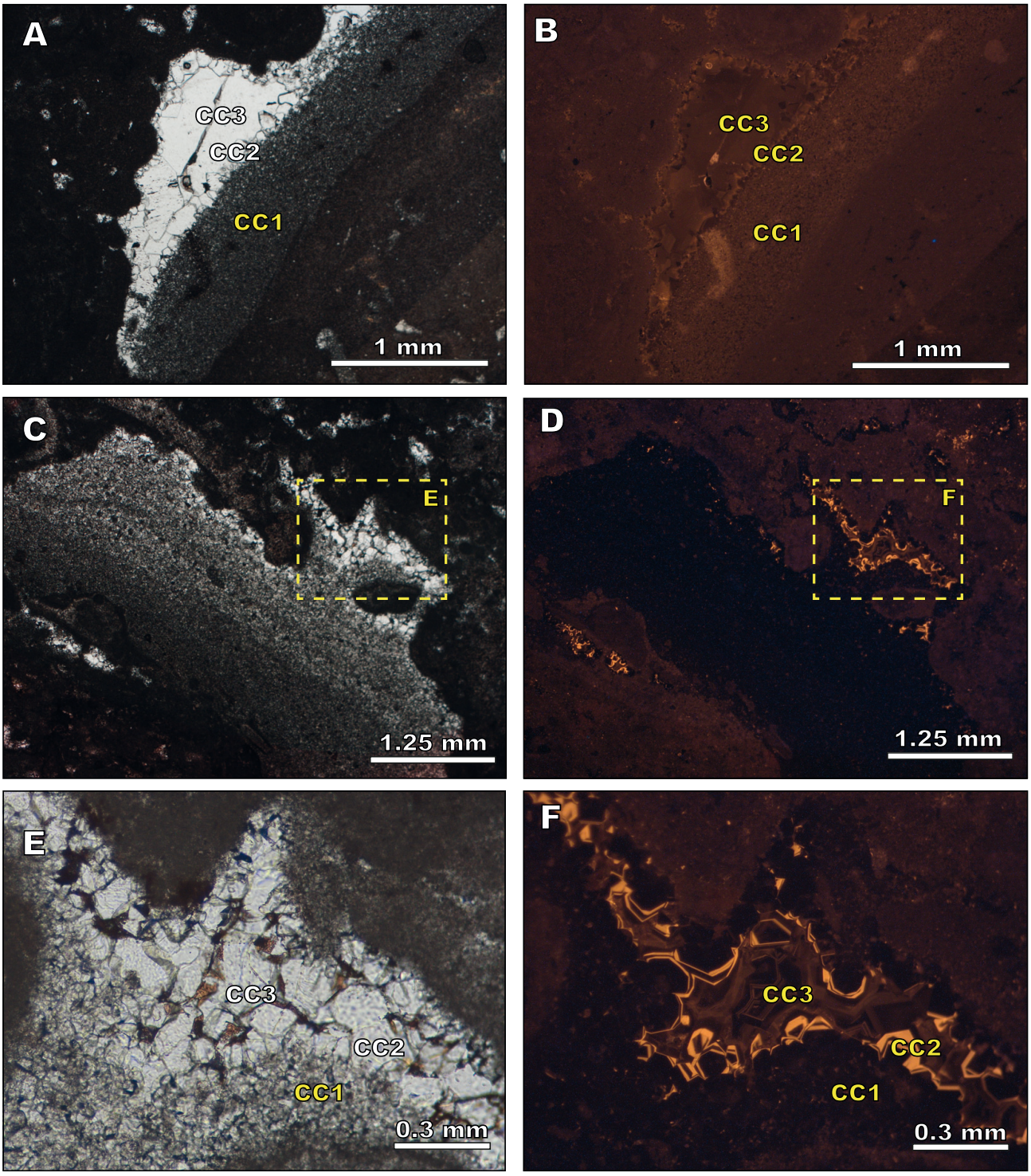

FIGURE 6. A, C, E) Pores with geopetal fillings indicating different phases of internal sediment and cement (CC). B, D, F) Corresponding cathodoluminescence images that display three phases, CC1: silt-sized internal sediment; CC2 and CC3: blocky cement. Refer to the text for further explanation.

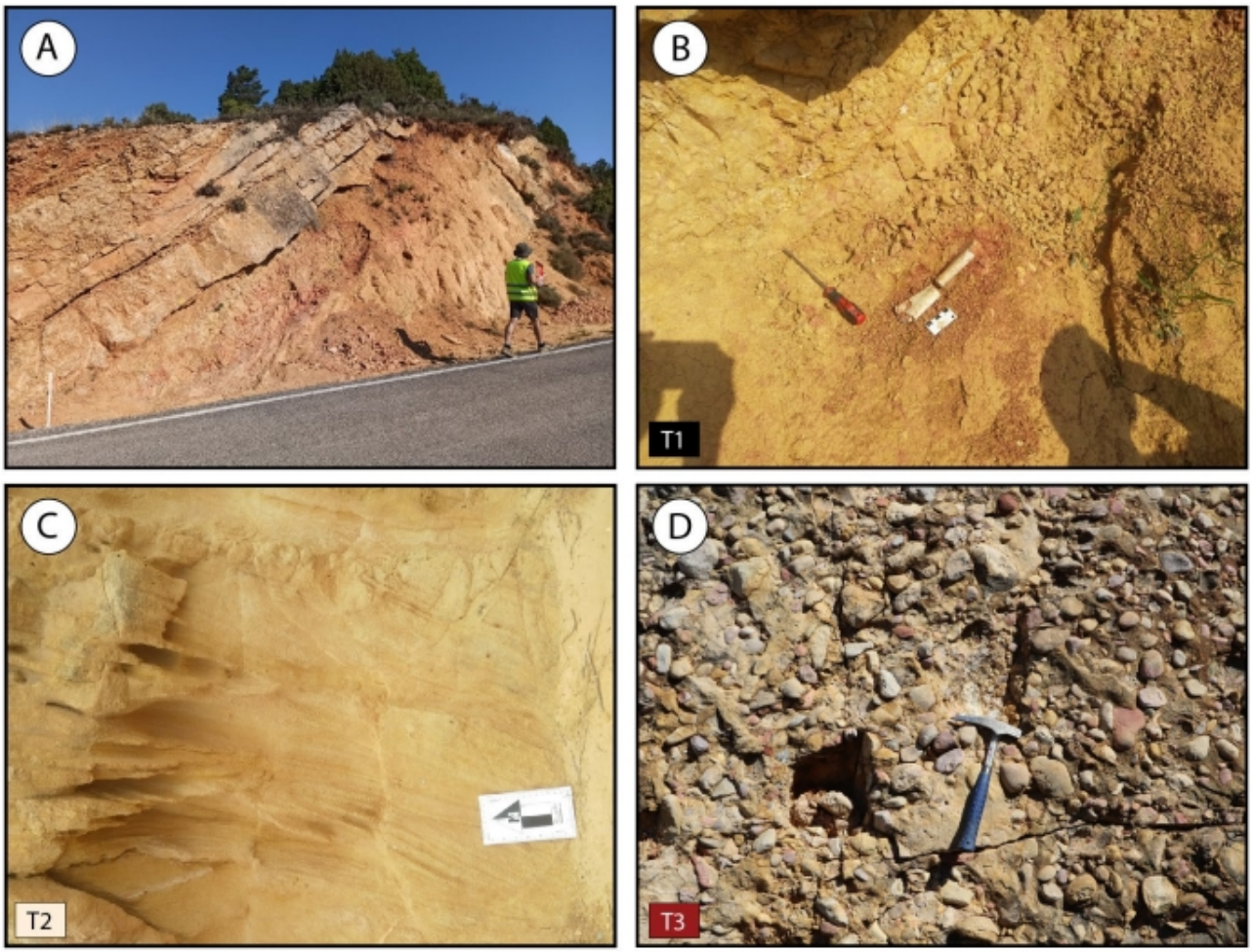

FIGURE 7. A) View of the Carretera Allueva fossil site, characterized by successive levels of reddish-brown sandstones, mudstones, and conglomerates with erosive bases. B) Facies T1: reddish-brown mudstone containing well-preserved dinosaur bones in the Carretera Allueva fossil site. C) Facies T2: fine-grained cross-bedded sandstones. D) Facies T3: massive conglomerate dominated by sub-rounded calcareous pebbles.

Thus, the commonly observed vertical transition from facies M1 to M2 (Fig. 3) may indicate an increase in water level in the system, leading to enhanced water motion during episodic high-energy events.

Among the desiccation features observed in the microbialite facies association, stromatactis-like structures are of particular interest. These structures mainly occur in carbonate mud, characterized by smooth, well-defined sharp bases, and variable sizes (Deelman, 1972; Hladil *et al.*, 2006, 2007). Plausible hypotheses for their origin include pores enlarged by dissolution, such as fenestral pores (Deelman, 1972), or the decay of organic precursors, such as microbial mats (Hladil *et al.*, 2007). The presence of different cement phases in stromatactis-like structures can provide insights into the paleoenvironmental conditions (Fig. 6). The first phase of geopetal infills (CC1) indicates precipitation under vadose conditions, while pore-lining equant calcite (CC2) and blocky cements (CC3) formed under phreatic conditions. These observations support the interpretation of fluctuating water levels in the characterized ponds and lakes.

Luminescence in the analysed samples from the A2 subunit is generally weak. The dark brown, non-luminescent CC1 cements probably formed in well-oxygenated waters, while the presence of yellow luminescent bands in CC2 (Fig. 6F) suggests the incorporation of Mn^{2+} into the calcite lattice under suboxic to anoxic conditions (Machel and Burton, 1991; Meyers, 1978). The dull luminescence of blocky CC3 calcite may indicate a further drop in oxygen levels, which facilitated the incorporation of Fe^{2+} into the carbonate growing crystal (Hiatt and Pufahl, 2014) or the return to more oxic conditions. These variations in luminescence are interpreted as being linked to hydrochemical variations driven by fluctuations in the water table.

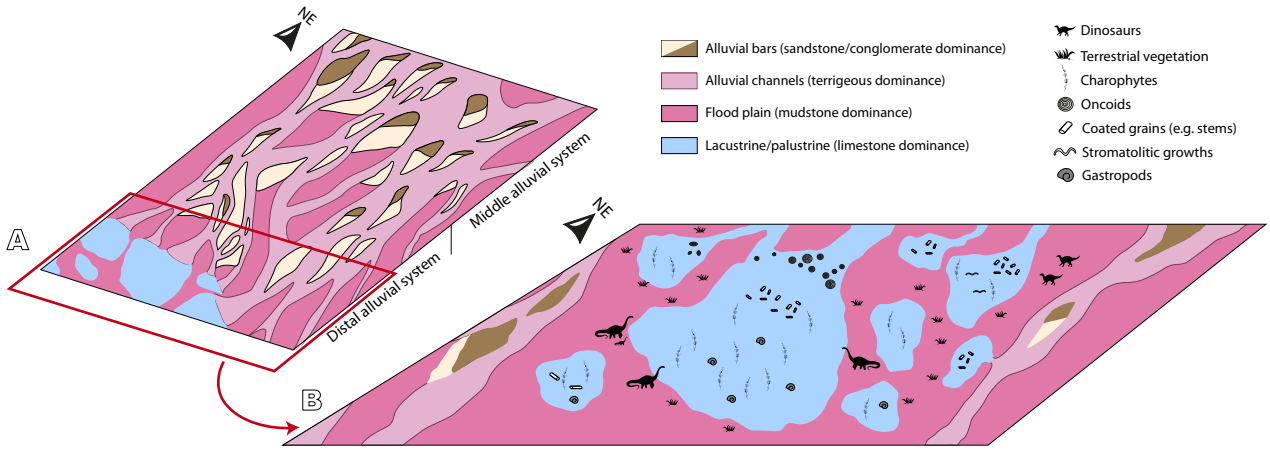

FIGURE 8. A schematic depositional model (not to scale) of the distal alluvial part of the Allueva Fm. Possible relationships between lithologies and the distribution of common grains are indicated.

MICROBIALITE ANALYSIS

Description

Different morphologies of microbialites have been identified (Figs. 9; 10), following the descriptions provided by Logan *et al.* (1964), Kennard and Burne (1989) and Riding (2000, 2008, 2011). For microscopic and lamination patterns, the classifications of Monty (1976) and Riding (2008) were used. Six distinct types of oncoids (O1–O6) were distinguished based on significant differences in external morphology and lamination.

Type O1 oncoids (found near the locality of Bea; Fig. 1C) are elongated (Fig. 9A), measuring between 2 and 4cm in length and 1 to 2cm in width. The central parts of these oncoids generally contain elongated voids, likely corresponding to degraded plant remains (phytoclastics). The concentric laminae are mostly undulatory to pseudocolumnar. Pronounced undulations with columnar-layered sectors indicate erosion and the re-precipitation of new laminae (Fig. 10A).

Type O2 oncoids (dominant between Gusepa and Carramatilla sections) are pseudospherical to ovoidal, with diameters ranging from 4 to 8cm. The nuclei are typically well-rounded intraclasts (Fig. 9B). The lamination is concentrically stacked, but asymmetric and randomly stacked laminae, with local pseudocolumnar to columnar patterns, are also common (Fig. 10B).

Type O3 oncoids (common in the Carramatilla section; Fig. 1C) are characterized by well-developed spherical to sub-spherical shapes, with concentrically stacked laminae (Fig. 9C). They range from 1 to 2cm to nearly 15cm, with dominant medium-sized oncoids (5-8cm). The nuclei are usually intraclasts of variable size and origin. Flat laminae are the most common; but undulatory and pseudocolumnar laminae can also be found, particularly in more elongated oncoids (Fig. 10C). Individual circular structures, 5-20μm in diameter (Fig. 10D), may be related to algal filaments.

Type O4 oncoids (Fig. 9D) are concentrated in the areas with higher terrigenous influence, particularly at the easternmost location of Cordal Allueva. They have cylindrical shapes and measure up to 20cm in length, and 1 to 5cm in width. Although these oncoids are reworked and highly fragmented, planar to pseudocolumnar fabrics can still be recognized (Fig. 10E).

Type O5 and O6 oncoids are also found at the Cordal Allueva site (Fig. 1C). Type O5 oncoids mainly consist of microbialite coatings (up to 1cm thick), surrounding a variety of nuclei, including cm-sized pebbles, dinosaur bones (Fig. 9E), and fragmented stromatolites (Fig. 9F). Type O6 oncoids, measuring 1 to 2cm in diameter, are formed by the aggregation of pre-existing oncoid fragments, that were bound together by new microbial coatings (Fig. 9G).

Isolated microbial growths up to 6cm thick and 1m long are locally found (Fig. 9H). Their laminae vary from flat to undulating, and occasionally exhibit a thrombolitic fabric (Fig. 10F). Certain lamination patterns resemble those of modern cyanobacteria. For example, wavy and domed lamination showing micrite filamentous bodies, extending upwards (Fig. 10G), is similar to *Phormidium*, whereas bush-like laminae, observed in certain tufa-like samples from facies M1 (Fig. 10H), resemble modern cyanobacteria of the genus *Dichothrix* (Freytet and Verrecchia, 1998; Zamarreño *et al.*, 1997).

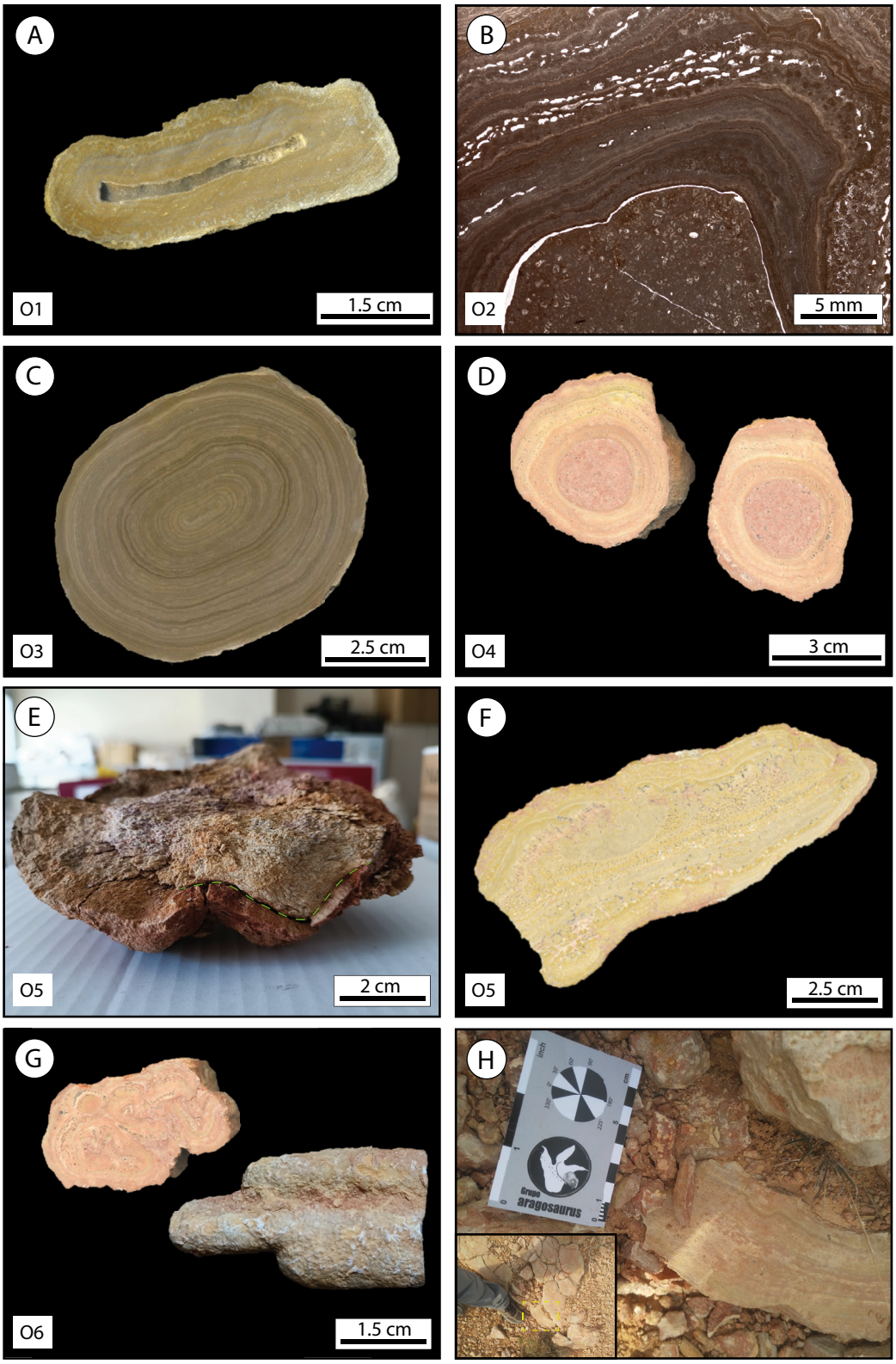

FIGURE 9. A) Elongated oncoid with concentrically stacked laminae. The central void corresponds to the original phytoclast nucleus. B) Concentrically stacked oncoid laminae with irregularities. Sparite-filled pores are aligned parallel to the lamination. The nucleus consists of a clast from facies association 1. C) Subspherical oncoid with concentrically stacked laminae. D) Cross-section of a cylindrical oncoid showing fragmented outer layers. E) Caudal vertebra of a sauropod dinosaur covered by a microbialite crust (indicated by the green line). F) Microbial coating on a fragment of a stromatolite exhibiting a thrombolitic fabric. G) Oncolite composed of pre-existing oncoid fragments, the cross-section shows an irregular lamination pattern. H) Isolated, elongated,and fragmented stromatolitic crust.

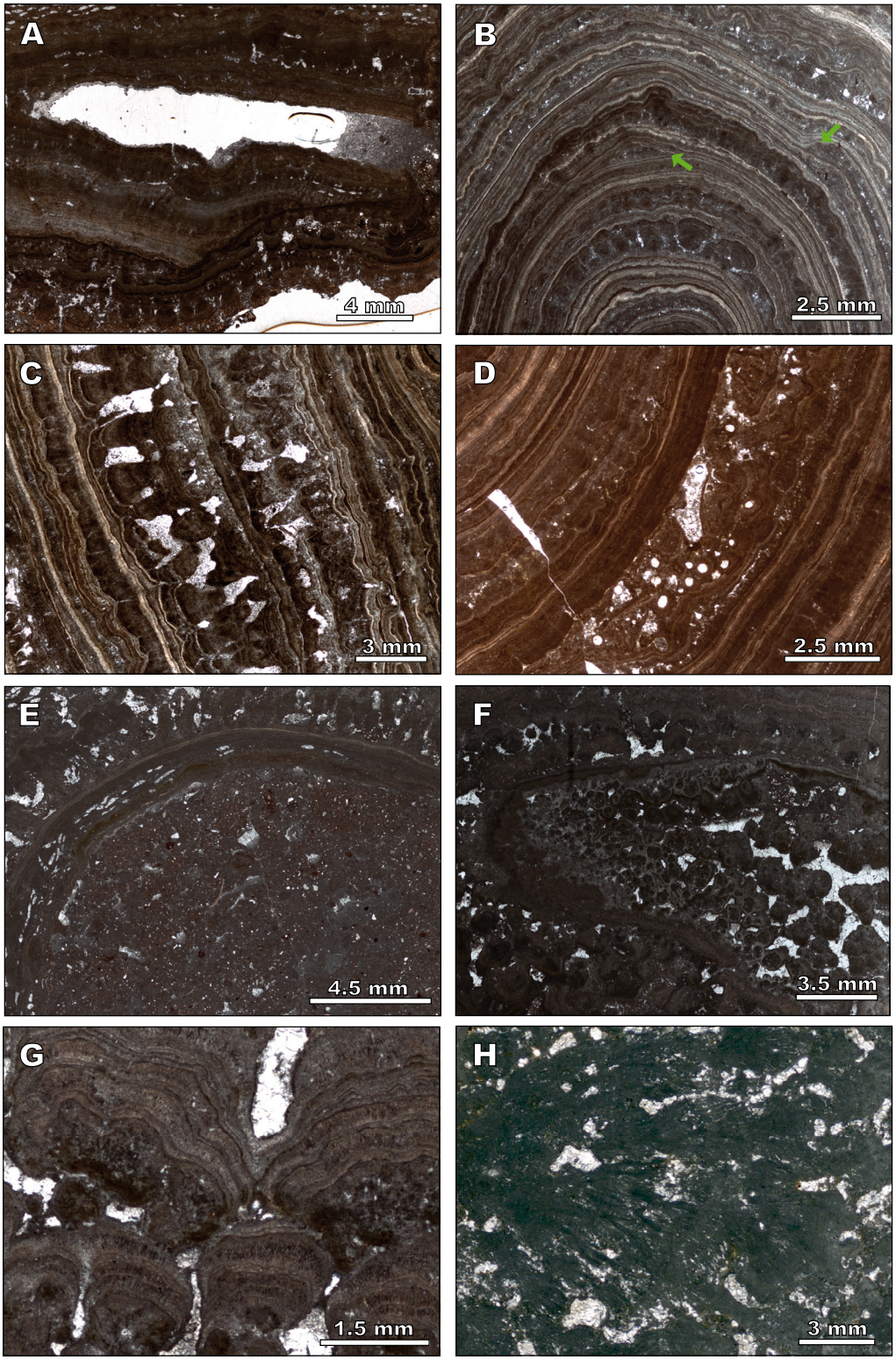

FIGURE 10. A) Concentrically stacked laminae with undulatory to pseudocolumnar patterns. The contact between eroded laminae and newly formed laminae is indicated by a green line. B) Concentrically stacked laminae showing irregularities. Significant lateral thickness variation, highlighted by the green line, while irregularities in the concentric laminae pattern are marked with green arrows. C) Concentrically stacked flat, undulatory and pseudocolumnar laminae. D) Well-developed, concentrically stacked flat and undulatory laminae. Chaotic patterns are present between the green lines, featuring pseudocolumnar arrangements and circular structures that may be related to algae. E) Altered concentrically stacked laminae exhibiting planar to pseudocolumnar patterns. Porosity parallel to the lamination is indicated by green lines. F) Thrombolitic fabric topped with a microbial coating featuring undulatory to pseudocolumnar patterns. G) Wave and domed-shaped lamination with micrite filaments extending upwards. H) Laminae radiate outwards forming a bush-like fabric that may be related to cyanobacteria.

Interpretation

Irregular and elongated morphologies of type O1 oncoids are associated with the shape of phytoclasts that constitute their nuclei (Fig. 9A). The identified sharp irregularities (Fig. 10A) are likely the result of high-energy events that eroded and fragmented the pre-existing oncoids. These features are similar to those observed in tufa-like deposits (M1 facies), and probably share a similar origin in small ponds colonized by plants and cyanobacteria, disconnected from the active sectors of the alluvial system (*e.g.* Parcerisa *et al.*, 2006).

Types O2 and O3 oncoids formed near the interface between channels and lakes, where constant high-energy conditions contributed to their well-developed concentricity and sphericity (Shapiro *et al.*, 2009; Torromé and Aurell, 2024). The concentrically stacked pattern and spherical shapes, dominant in type O3 oncoids are indicative of permanently submerged conditions and continuous water motion (*e.g.* Ginsburg, 1960; Logan *et al.*, 1964). In contrast, type O2 oncoids are less spherical and display numerous unconformities and irregularities in their laminae, indicating periods of low turbulence that hindered the development of well-defined concentric lamination (Logan *et al.*, 1964).

Type O4, O5 and O6 oncoids, which are frequently eroded and fragmented, likely originated in isolated ponds adjacent to active channels. These areas are expected to experience a higher frequency of high-energy events, resulting in significant terrigenous input (*e.g.* Arenas *et al.*, 2015; Berra *et al.*, 2019; Plaziat, 1984). Furthermore, the isolated oncoids found within the associated conglomeratic levels indicate erosion and reworking, processes that commonly occur in alluvial settings (*e.g.* Berra *et al.*, 2019; Parcerisa *et al.*, 2006).

Stromatolites develop in low energy settings (Gebelein, 1976; Logan *et al.*, 1964; Nickel, 1983; Riding, 2011), and their relative scarcity in the Allueva Fm. compared to oncoids can be attributed to the constant reactivation of alluvial channels. Non-fragmented stromatolitic forms are mostly preserved in areas with higher water levels and lower energy (Carramatilla and Gusepa sections; Fig. 1C), which are more conducive to their proliferation (*e.g.* Arenas *et al.*, 2015; Martín-Bello *et al.*, 2019; Petryshyn *et al.*, 2012; Riding, 2011). Stromatolites develop large and pronounced domes as water depth increases (Awramik and Buchheim, 2015; Roche *et al.*, 2018). However, most of the observed stromatolites have flat shapes, with wavy and pseudocolumnar laminations. These features are consistent with their formation in shallow waters (Martín-Bello *et al.*, 2019).

Lamination patterns in oncoids

A wide spectrum of lamination patterns can be distinguished in the studied oncoids, ranging from flat- to columnar-layered structures (Fig. 10). A simple lamina in a microbialite is defined as a layer less than 10mm thick, characterized by a uniform texture and clearly separated from other laminae by sharp or gradual changes in color and/or texture (Arenas and Jones, 2017). The simple laminae of the studied oncoids are mostly composed of micrite, with subordinate sparite. Following the nomenclature of Martín-Bello *et al.* (2019), four types of simple laminae are distinguished (Fig. 11A): i) Light Dense (LD), with laminae ranging from 0.1 to 0.5mm, characterized by whitish-brown to light brown micrite; ii) Dark Dense (DD), with laminae ranging from 0.1 to 1mm, characterized by brown to dark brown micrite; iii) Dark Porous (DP), with laminae ranging from 0.5 to 2.5mm, characterized by dark colors, lighter than those typical of DD laminae due to their clotted-micropeloidal texture and iv) Sparite (Sp), with laminae ranging from 0.1 to 0.25mm, characterized by larger calcite crystals that grew perpendicular to the lamination.

Simple laminae can be grouped into four different types of composite laminae (Fig. 11B): i) Dark Composite Laminae (DCL) formed by successive DD laminae intercalated with LD laminae; ii) Dark Porous Composite Laminae (DPCL) formed by the stacking of dark porous laminae intercalated with LD laminae; iii) Light Composite Laminae (LCL) characterized by a predominance of LD laminae intercalated with DD laminae; iv) In some oncoids where Sp laminae are present, these composite laminae are referred to as LCL + Sp.

Following the classification of Monty (1976), four lamination patterns are differentiated in the studied microbialites (Fig. 11C). Composite alternating lamination is categorized into three different variations of DCL-LCL alternation: DCL-dominated, LCL-dominated (which sometimes exhibits Sp laminae), and those with nearly equal in presence of both types. No distinct thickening or thinning patterns were observed in these three types of composite alternating laminae. The only observed cyclothemic lamination consists of a three-laminae succession in the form of DCL-LCL-DPCL alternation (Fig. 11C). Additionally, SEM analysis revealed no compositional differences between microbialite layers or between different phases of cementation, as all layers are composed of low magnesium calcite.

Significance of lamination patterns

In previous studies (Casanova, 1986, 1994; Frantz *et al.*, 2014), Dark Porous laminae (DP) have been associated

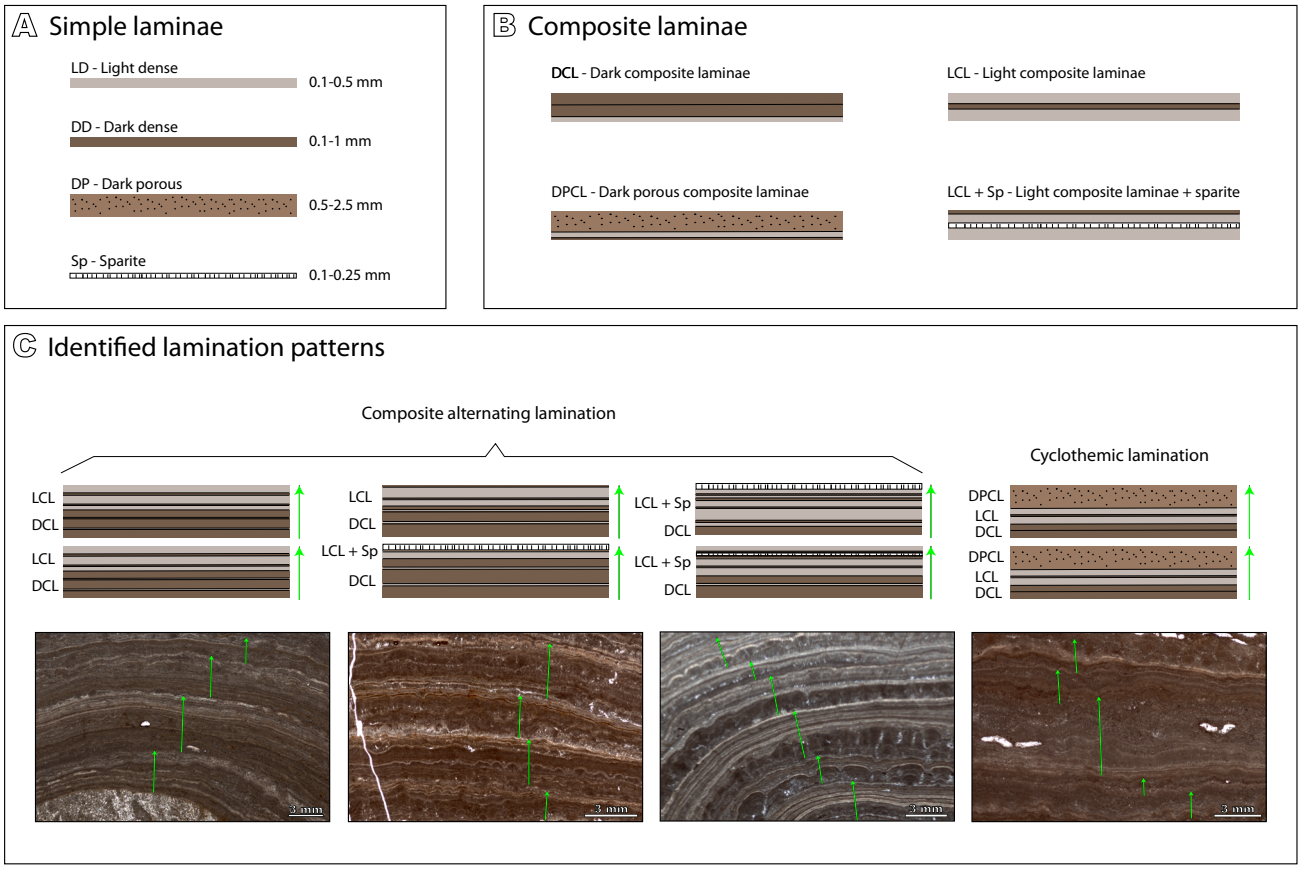

FIGURE 11. A) Different types of simple laminae: Light Dense (LD), Dark Dense (DD), Dark Porous (DP) and Sparite (Sp). B) Different types of composite laminae: Dark Composite Laminae (DCL), Light Composite Laminae (LCL) and Dark Porous Composite Laminae (DPCL). C) Two types of lamination patterns: Cyclothemic Lamination (DCL-LCL-DPCL) and Composite alternating Lamination (DCL-LCL). Figure based on Martín-Bello *et al.* (2019).

with cool and humid conditions, while dense laminae (LD, DD) are usually related to drier environments. On the other hand, the genesis of Sp remains poorly understood, but it is often attributed to early diagenetic processes (Freytet and Verrecchia, 1999) or to the preservation of primary textures (Grotzinger and Knoll, 1999). In the oncoids from the Allueva Fm., the sparite laminae appears to be primary and may be linked to microbial activity (Freytet and Verrecchia, 1998).

The alternation of light and dark laminae in microbialites has been documented in a wide range of environments (Kano *et al.*, 2007; Martín-Bello *et al.*, 2019; Monty, 1976; Zamarreño *et al.*, 1997). These alternations have traditionally been linked to variations in temperature, precipitation, and evaporation within the environments (Casanova, 1994; Woo *et al.*, 2004). The time span represented by each lamina cycle has been widely debated (Casanova, 1994; Suarez-Gonzalez *et al.*, 2014). The formation of a lamina-pair is often interpreted as representing a single year of growth, based on textural and geochemical evidence (Arp *et al.*, 2010; Kano *et al.*, 2007; Riding, 2000; Seong-Joo *et al.*, 2000). However, other studies suggest that a few months may be sufficient to develop multiple laminae due to both periodic and non-periodic factors (Drysdale and Gillieson, 1997; Gradzinski, 2010; Ordóñez *et al.*, 1980; Vázquez-Urbez *et al.*, 2010).

ISOTOPIC ANALYSIS ($\delta^{18}O$ AND $\delta^{13}C$)

Isotopic analysis ($\delta^{18}O$ and $\delta^{13}C$) is a valuable tool for paleoenvironmental interpretation, particularly for assessing climatic and hydrological conditions (*e.g.* Teranes and McKenzie, 2001; Leng and Marshall, 2004). Torromé and Aurell (2024) presented the $\delta^{18}O$/$\delta^{13}C$ isotopic signal from Allueva oncoids by analyzing successive layers of a single oncoid (Fig. 12). In the present study, 14 bulk carbonate samples were collected from the Carramatilla log (Fig. 13) to determine the vertical evolution of isotopic values. The results show low variation in $\delta^{13}C$ values (min: –5.5‰, max: –3.6‰) and a relatively narrow range of $\delta^{18}O$ values (min. –5.6‰, max: –4.4‰), with no significant covariation between $\delta^{13}C$ and

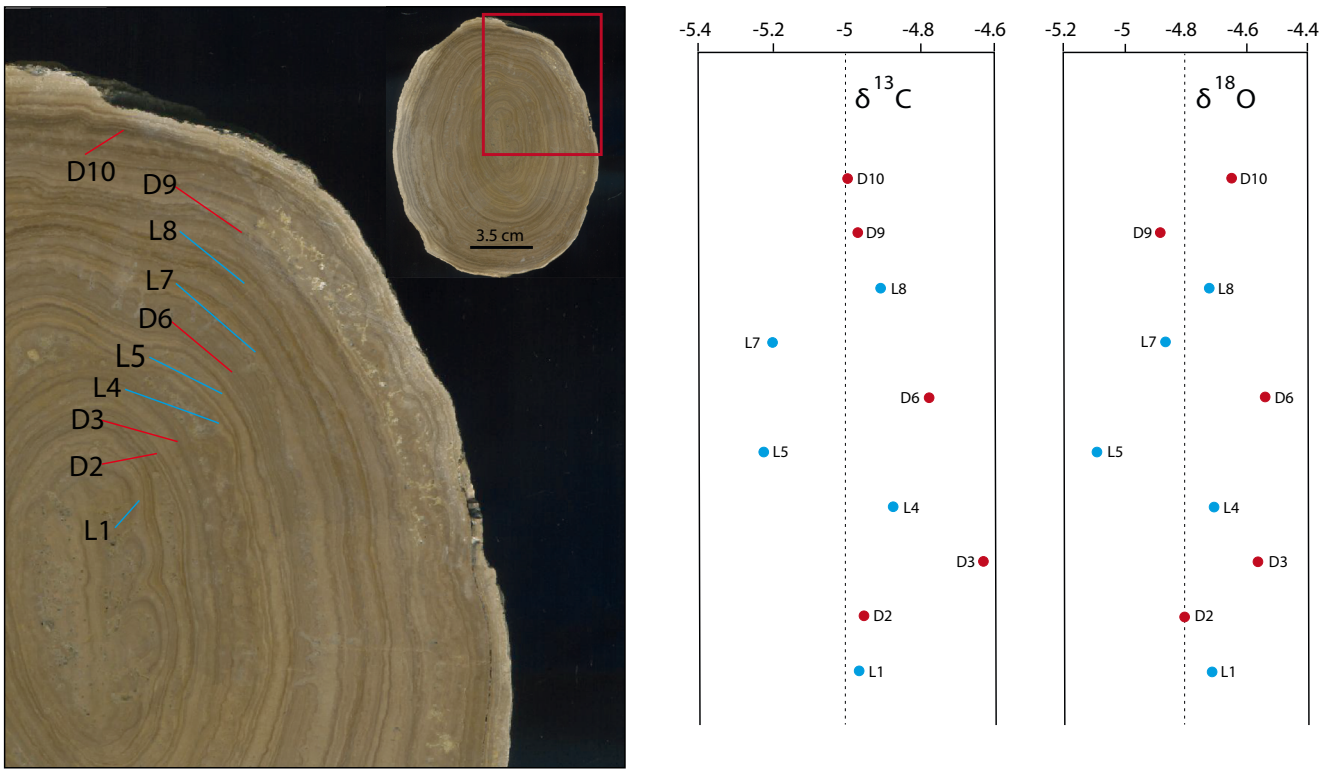

FIGURE 12. An oncoid from Carramatilla highlighting the sampled light (blue) and dark (red) micritic laminae. The corresponding stable isotopic profiles of $\delta^{13}C$ and $\delta^{18}O$ are displayed in the right columns. Data sourced from Torromé and Aurell (2024).

$\delta^{18}O$ (r= 0.22; Fig. 14). The $\delta^{18}O$ values show a slight vertical trend, increasing upwards, while $\delta^{13}C$ values show a sharp decrease in the first meters of the log, before stabilizing further up (Fig. 13).

The isotopic results obtained are within the range of freshwater lake carbonates as defined by Leng and Marshall (2004) and are comparable to those reported for other fluvial-lacustrine systems (Arenas *et al.*, 2007, 2015; Ordóñez *et al.*, 2005). Additionally, the results are consistent with those of limestones of meteoric origin (Andrews, 2006; Leng and Marshall, 2004). The $\delta^{18}O$ variation, less than 1‰, is characteristic of lakes and ponds with short water residence times, where evaporation processes have a limited impact on $\delta^{18}O$ variation (Leng and Marshall, 2004).

Negative $\delta^{18}O$ values are typically associated with humid conditions (Leng and Marshall, 2004). Although the values obtained in this study are negative, they are not low enough to suggest intense humid conditions, but rather indicate sub-humid to humid environments. However, the slight increase in $\delta^{18}O$ values (Fig. 13) may point to a gradual decrease in humidity over time. Conversely, lower $\delta^{13}C$ values are often linked to a decline in organic activity (McKenzie, 1985; Platt, 1989).

The isotopic results also provide information into the oncoid lamination patterns (Andrews and Brasier, 2005; Casanova, 1986, 1994). Although the isotopic values do not exhibit significant variations, light dense laminae show slightly lower $\delta^{18}O$ and $\delta^{13}C$ values compared to the dark dense laminae (Fig. 12). This trend has been observed in previous studies (Leng and Marshall, 2004; Martín-Bello *et al.*, 2017, 2019), suggesting that dark laminae correspond to drier conditions, whereas light laminae may reflect more humid periods.

DISCUSSION

Hydrological controls

The palustrine-lacustrine environments studied in this work developed a few kilometers from the uplifted source area on the southern flank of the Montalbán anticline (Aurell *et al.*, 2022; Gónzalez and Pérez, 2018; Fig. 1A). The progressive increase in the sedimentation rate observed in the Allueva Fm. shows the coeval progressive uplift of this source area, which may have led to a gradual increase in the gradient of the alluvial system during the sedimentation of subunit A2 (Aurell *et al.*, 2022).

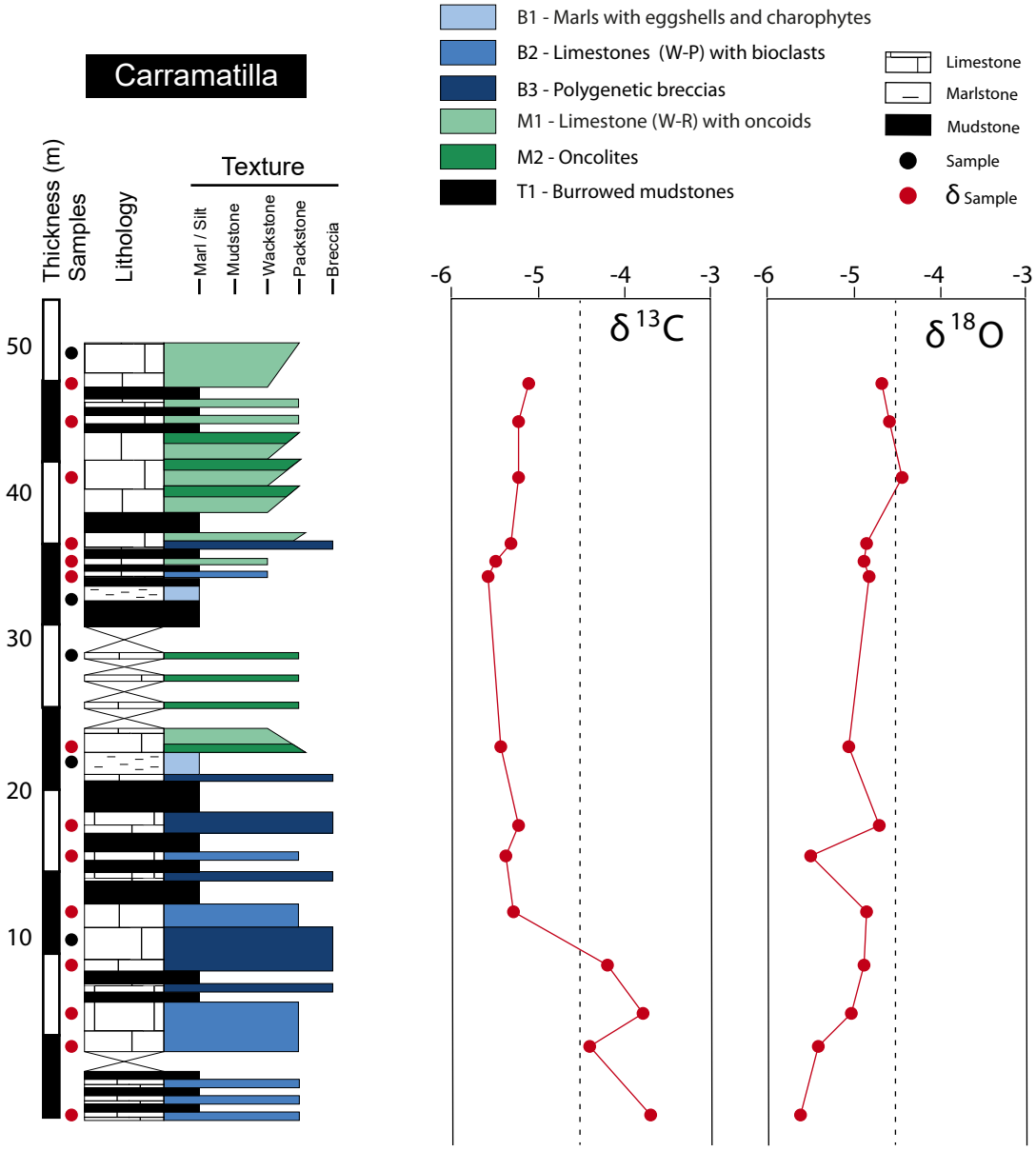

FIGURE 13. j Stratigraphic log of the Carramatilla section, showing the location of the bulk carbonate samples used for isotopic analysis (red dots). The $\delta^{13}C$ and $\delta^{18}O$ data are displayed in the right columns.

In the studied succession, the overall alternation of bioclastic to microbialite facies associations (Fig. 3) can be attributed to episodic fluctuations in water influx. High-energy stages with significant water input would have favored the development of oncoids over stromatolites (Gebelein, 1976; Logan *et al.*, 1964; Nickel, 1983), while reducing the proliferation of charophytes and gastropods in the ponds (*e.g.* Logan *et al.*, 1964; Shapiro *et al.*, 2009). In contrast, low energy stages with reduced water influx into lakes and ponds, would have promoted the proliferation of gastropods and charophytes, as well as the formation of breccias, both characteristic of the bioclastic facies association (*e.g.* Alonso-Zarza and Wright, 2010; Plaziat, 1984).

Tufa-like deposits are commonly associated with springs (Andrews, 2006). However, such an origin is unlikely in the studied alluvial system. Spring-formed limestones are often linked to karst systems and aquifers, where reduced evaporation results in significantly lower $\delta^{18}O$ values (<-12‰; Andrews, 2006). Accordingly, the tufa deposits of the Allueva Fm. were more likely developed in ponds or abandoned channels within the alluvial system, where intense microbial precipitation occurred (*e.g.* Alonso-Zarza and Wright, 2010; Arenas *et al.*, 2007; Vázquez-Urbez *et al.*, 2013).

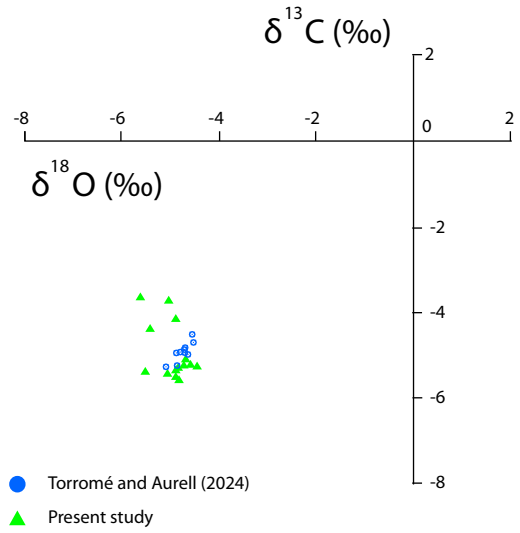

FIGURE 14. $\delta^{18}O$ and $\delta^{13}C$ plot of the samples from the Carramatilla log (green) and from a single oncoid (blue).

Climatic controls

The stable isotope composition of the studied lacustrine-palustrine carbonates suggests deposition under sub-humid conditions. However, the local presence of gypsum (Fig. 4F) in the upper part of the studied succession indicates the presence of episodic arid or semi-arid conditions (*e.g.* Sanz *et al.*, 1995). It is therefore likely that alternating periods of sub-humid and semi-arid conditions occurred, as has been reported in other lacustrine environments (*e.g.* Platt and Wright, 1991; Sanz *et al.*, 1995; Torromé *et al.*, 2023).

Climatic fluctuations may also be reflected in the lamination patterns observed in the oncoids of the Allueva Fm. (*e.g.* Hofmann, 1973; Monty, 1976; Petryshyn *et al.*, 2012; Frantz *et al.*, 2014). Composite laminations typically develop over periods longer than a single year, reflecting alternating humid and dry phases. In this context, as inferred from individual laminae, DCL may correspond to drier conditions, while LCL may indicate more humid periods. These temporal and climatic interpretations are tentative and require further validation through high-resolution carbon and oxygen stable isotope analyses, as well as detailed periodicity studies of the lamination patterns. Furthermore, it is critical to recognize the inherent challenges in interpreting isotopic data without making significant assumptions (Leng and Marshall, 2004), particularly when using samples derived from bulk rock.

The possible impact of the late Campanian ecological crisis

Microbialites may begin to develop following periods of ecological crisis (Sheehan and Harris, 2004). For instance, the extensive giant microbialites found in the Tremp Fm. of the South-Central Pyrenees have been linked to the K/Pg global crisis (Astibia *et al.*, 2012). Similarly, the microbialites from the Allueva Fm. could potentially be associated with the middle-late Campanian ecological crisis described elsewhere. Some authors have reported a late Campanian-early Maastrichtian ecological crisis that led to a faunal turnover across the Ibero-Armorican landmass, primarily affecting herbivorous dinosaurs (Csiki-Sava *et al.*, 2015; Le Loeuff *et al.*, 1994; Sellés and Vila, 2015; Vila *et al.*, 2016). However, this turnover was related to paleogeographic changes that favored the introduction of new immigrant taxa, resulting in altered survival dynamics (Csiki-Sava *et al.*, 2015; Isasmendi *et al.*, 2022; Prieto-Márquez *et al.*, 2013). Additionally, Ikejiri *et al.* (2020) identified a middle Campanian crisis based on a decline in marine vertebrate fauna. The causes of this global event remain uncertain, with hypotheses including a globally recorded sea-level regression (Haq, 2014), faunal changes in plankton, marine anoxia, or ocean acidification (Ikejiri *et al.*, 2020). Although evidence suggests this event occurred, it primarily seems to have impacted marine environments, with its influence on continental environments remains to be demonstrated.

CONCLUSIONS

The carbonates and microbialites found locally in the Allueva Fm. developed in an area of lacustrine-palustrine sedimentation with fluctuating water levels. This area was part of an extensive, low-gradient alluvial system dominated by fluvial processes and fed by carbonate-rich meteoric waters.

Three facies associations were identified, each corresponding to a specific part of the depositional system: i) A bioclastic facies association comprising intensely bioturbated marlstone and limestone beds rich in charophytes and gastropods; ii) A microbialite facies association characterized by extensive tufa-like deposits, stromatolites and oncoids; iii) A terrigenous facies association consisting of alternating conglomerates, sandstones and mudstones, formed within a braided fluvial system that migrated across a broad floodplain.

Among the identified microbialites, oncoids are significantly more abundant than stromatolites, and six distinct types (O1–O6) are recognized. Oncoid of type O1 and O4-O6 show characteristics indicative of formation in small ponds or abandoned channels. In contrast, oncoids of type O2 and O3 exhibit features associated with areas of consistent turbulence, such as at the interface between channels and lakes.

The $\delta^{13}C$ values (ranging from –5.6‰ to –3.7‰) and $\delta^{18}O$ values (ranging from –5.6‰ to –4.5‰) falls within the typical range for freshwater lake carbonates, indicating sub-humid climatic conditions. The occurrence of gypsum in the upper levels of the studied unit suggests a gradual shift toward a more arid climate, which is also reflected in the upward trend in $\delta^{18}O$ values. This climatic shift likely led to seasonal fluctuations between sub-humid and semi-arid conditions, which played an important role in the cyclicity of microbialite lamination. Darker laminae (associated with heavier isotopic values) likely correspond to more arid conditions, while lighter laminae (associated with lighter values) indicate more humid periods.

The Allueva Fm. presents several features that may indicate an ecological crisis during the late Campanian, including extensive microbialite development at an outcrop scale of over 10 km and evidence of faunal turnover. This faunal turnover has previously been linked to the influx of immigrant taxa, driven by regional paleogeographic changes during the late Campanian and early Maastrichtian. Correlating these changes with the middle Campanian crisis is more difficult, as that event primarily impacted marine environments.

ACKNOWLEDGMENTS

This paper is funded by projects PID2021-122612OBI00 and Group E18 (Aragosaurus: Geological Resources and Paleoenvironments), supported by the Ministerio de Ciencia e Innovación, the European Regional Development Fund, and the Government of Aragón. The research conducted by Diego Torromé is supported by a DGA Grant from the Aragón department of science, university, and society of knowledge. We are grateful for the resources provided by the Servicio General de Apoyo a la Investigación-SAI, Universidad de Zaragoza, and for the valuable recommendations and advice from Leticia Martín Bello. The contributions of A. Košir and A. Martín Pérez were supported by the project J1-50028 from the Slovenian Research and Innnovation Agency (ARIS). We also extend our gratitude to David Parcerisa, Cristina Sequero and the Editor, Telm Bover, whose revisions significantly improved the original version of the manuscript.

REFERENCES

Allen, J.R.L., 1983. Gravel overpassing on humpback bars supplied with mixed sediment: examples from the Lower Old Red Sandstone, southern Britain. Sedimentology, 30(2), 285-294. DOI: https://doi.org/10.1111/j.1365-3091.1983.tb00671.x

Alonso-Zarza, A.M., Calvo, J.P., 2000. Palustrine sedimentation in an episodically subsiding basin: the Miocene of the northern Teruel Graben (Spain). Palaeogeogaphy, Palaeoclimatology, Palaeoecology, 160, 1-21. DOI: https://doi.org/10.1016/S0031-0182(00)00041-9

Alonso-Zarza, A.M., Wright, V.P., 2010. Palustrine carbonates. In: Alonso-Zarza, A.M., Tanner, L.H. (eds.). Carbonates in continental settings. Developments in Sedimentology, 61, 103-131. DOI: https://doi.org/10.1016/S0070-4571(09)06102-0

Andres, M.S., Reid, R.P., 2006. Growth morphologies of modern marine stromatolites: A case study from Highborne Cay, Bahamas. Sedimentary Geology, 185, 319-328. DOI: https://doi.org/10.1016/j.sedgeo.2005.12.020

Andrews, J.E., 2006. Palaeoclimatic records from stable isotopes in riverine tufas: synthesis and review. Earth-Science Reviews, 75(1-4), 85-104. DOI: https://doi.org/10.1016/j.earscirev.2005.08.002

Andrews, J.E., Brasier, A.T., 2005. Seasonal records of climatic change in annually laminated tufas: Short review and future prospects. Journal of Quaternary Science, 20, 411-421. DOI: https://doi.org/10.1002/jqs.942

Arenas, C., Jones, B., 2017. Temporal and environmental significance of microbial lamination: Insights from Recent fluvial stromatolites in the River Piedra, Spain. Sedimentology, 64, 1597-1629. DOI: https://doi.org/10.1111/sed.12365

Arenas, C., Cabrera, L., Ramos, E., 2007. Sedimentology of tufa facies and continental microbialites from the Palaeogene of Mallorca Island (Spain). Sedimentary Geology, 197, 1-27. DOI: https://doi.org/10.1016/j.sedgeo.2006.08.009

Arenas, C., Piñuela, L., García□Ramos, J.C., 2015. Climatic and tectonic controls on carbonate deposition in syn□rift siliciclastic fluvial systems: A case of microbialites and associated facies in the Late Jurassic. Sedimentology, 62(4), 1149-1183. DOI: https://doi.org/10.1111/sed.12182

Arenas-Abad, C., Vázquez-Urbez, M., Pardo-Tirapu, G., Sancho-Marcén, C., 2010. Fluvial and associated carbonate deposits. In: Alonso-Zarza, A.M., Tanner, L.H. (eds). Carbonates in Continental Settings: Facies, Environments and Processes. Developments in Sedimentology, 61, 133-175.

Arp, G., Bissett, A., Brinkmann, N., Cousin, S., deBeer, D., Friedl, T., Mohr, K.I., Neu, T.R., Reimer, A., Shiraishi, F., Stackebrandt, E., Zippel, B., 2010. Tufa-forming biofilms of German karstwater streams: Microorganisms, exopolymers, hydrochemistry and calcification. In: Pedley, M., Rogerson, M. (eds.). Tufas and Speleothems: Unravelling the Microbial and Physical Controls. London, The Geological Society, 336 (Special Publications), 83-118. DOI: https://doi.org/10.1016/S0070-4571(09)06103-2

Astibia, H., López-Martínez, N., Elorza, J., Vicens, E., 2012. Increasing size and abundance of microbialites (oncoids) in connection with the K/T boundary in non-marine environments in the South Central Pyrenees. Geologica Acta, 10(3), 209-226. DOI: https://doi.org/10.1344/105.000001770

Aurell, M., Fregenal-Martínez, M., Bádenas, B., Muñoz-García, M.B., Élez, J., Meléndez, N., De Santisteban, C., 2019. Middle Jurassic-early cretaceous tectonosedimentary evolution of the southwestern Iberian Basin (central Spain): Major

palaeogeographical changes in the geotectonic framework of the Western Tethys. Earth Science Reviews, 199, 102983. DOI: https://doi.org/10.1016/j.earscirev.2019.102983

Aurell, M., Torromé, D., Gasca, J.M., Calvín, P., Pérez-Pueyo, M., Parrilla-Bel, J., Medrano-Aguado, E., Martín-Closas, C., Vicente, A., Sierra-Campos, P., Canudo, J.I., 2022. Latest Cretaceous palaeogeographic evolution of northeast Iberia: Insights from the Campanian continental Montalbán subbasin (Spain). Earth-Science Reviews, 104251. DOI: https://doi.org/10.1016/j.earscirev.2022.104251

Awramik, S.M., Buchheim, H.P., 2015. Giant stromatolites of the Eocene Green River Formation (Colorado, USA). Geology, 43(8), 691-694. DOI: https://doi.org/10.1130/G36793.1

Berra, F., Felletti, F., Tessarollo, A., 2019. Oncoids and groundwater calcrete in a continental siliciclastic succession in a fault-controlled basin (Early Permian, Northern Italy). Facies, 65, 1-19. DOI: https://doi.org/10.1007/s10347-019-0580-5

Bosence, D., 2012. Mesozoic, syn-rift, non-marine, microbialites from the Wessex Basin, UK. American Association of Petroleum Geologists (AAPG) Hedberg Conference, Microbial Carbonate Reservoir Characterization, 1-3.

Casanova, J., 1986. Les stromatolites continentaux: Paléoecologie, paléohydrologie, paléo-climatologie. Application au Rift Gregory. PhD Thesis. Marseille, Université Marseille-Luminy, 256pp.

Casanova, J., 1994. Stromatolites from the East African Rift: A synopsis. In: Bertrand-Sarfati, J., Monty, C. (eds.). Phanerozoic Stromatolites II. Dordrecht, Kluwer Academic Publishers, 193-226.

Casas, A.M., Casas, A., Pérez, A., Tena, S., Barrier, L., Gapais, D., Nalpas, T., 2000. Syn-tectonic sedimentation and thrust-and-fold kinematics at the intra-mountain Montalbán Basin (northern Iberian Chain, Spain). Geodinamica Acta, 13, 1-17. DOI: https://doi.org/10.1016/S0985-3111(00)00105-4

Choi, S., Han, S., Kim, N.H., Lee, Y.N., 2018. A comparative study of eggshells of Gekkota with morphological, chemical compositional and crystallographic approaches and its evolutionary implications. PLoS One, 13(6), e0199496. DOI: https://doi.org/10.1371/journal.pone.0199496

Cloud, P.E., 1942. Notes on stromatolites. American Journal of Science, 240, 363-379. DOI: https://doi.org/10.2475/ajs.240.5.363

Csiki-Sava, Z., Buffetaut, E., □si, A., Pereda-Suberbiola, X., Brusatte, S.L., 2015. Island life in the Cretaceous-faunal composition, biogeography, evolution, and extinction of land-living vertebrates on the Late Cretaceous European archipelago. ZooKeys, 469, 1-161. DOI: https://doi.org/10.3897/zookeys.469.8439

Deelman, J.C., 1972. On mechanisms causing birdseye structures. Neues Jahrbuch für Geologie und Paläontologie, 10, 582-595.

Drysdale, R., Gillieson, D., 1997. Micro-erosion meter measurements of travertine deposition rates: A case study from louie creek, Northwest Queensland, Australia. Earth Surface Processes and Landforms, 22, 1037-1051. DOI: https://doi.org/10.1002/(SICI)1096-9837(199711)22:11%3C1037::AID-ESP800%3E3.0.CO;2-X

Dunham, R.J., 1962. Classification of carbonate rocks according to depositional textures. American Association of Petroleum Geologists Bulletin, 1, 108-121.

Floquet, M., 1991. La plate-forme Nord-castillane au Crétacé supérieur (Espagne). Arrière-pays ibérique de la marge passive basco-cantabrique. Sédimentation et Vie. PhD Thesis. University of Dijon, 925pp.

Flügel, E., 2004. Microfacies data: fabrics. In: Flügel, E. (ed). Microfacies of Carbonate Rocks: Analysis, Interpretation and Application. Berlin, Heidelberg, Springer, 177-242.

Frantz, C.M., Petryshyn, V.A., Marenco, P.J., Tripati, A., Berelson, W.M., Corsetti, F.A., 2014. Dramatic local environmental change during the Early Eocene Climatic Optimum detected using high resolution chemical analyses of Green River Formation stromatolites. Palaeogeography, Palaeoclimatology, Palaeoecology, 405, 1-15. DOI: https://doi.org/10.1016/j.palaeo.2014.04.001

Freeman, T.O.M., Rosell, J., Obrador, A., 1982. Oncolites from lacustrine sediments in the Cretaceous of north□eastern Spain. Sedimentology, 29(3), 433-436. DOI: https://doi.org/10.1111/j.1365-3091.1982.tb01806.x

Freytet, P., Plaziat, J.C., 1982. Continental carbonate sedimentation and pedogenesis-Late Cretaceous and Early Tertiary of southern France. Contributions to Sedimentology, 12, 1-123.

Freytet, P.,Verrecchia, E.P., 1998. Freshwater organisms that build stromatolites: a synopsis of biocrystallization by prokaryotic and eukaryotic algae. Sedimentology, 45(3), 535-563. DOI: https://doi.org/10.1046/j.1365-3091.1998.00155.x

Freytet, P., Verrecchia, E.P., 1999. Calcitic radial palisadic fabric in freshwater stromatolites: diagenetic and recrystallized feature or physicochemical sinter crust? Sedimentary Geology, 126(1-4), 97-102. DOI: https://doi.org/10.1016/S0037-0738(99)00034-2

García, A., Chivas, A.R., 2006. Diversity and ecology of extant and Quaternary Australian charophytes. Cryptogamie Algologie, 27, 323-340.

García, A., Mas, R., Segura, M., Carenas, B., García-Hidalgo, J.F., Gil, J., Alonso, A., Aurell, M., Bádenas, B., Benito, M.I., Meléndez, A., Salas, R., 2004. Segunda fase de post-rifting: Cretácico Superior. In: Vera, J.A. (ed.). Geología de España. Madrid, Sociedad Geológica de España and Instituto Geológico y Minero de España, 510-522.

Gebelein, C.D., 1976. Open marine subtidal and intertidal stromatolites (Florida, the Bahamas and Bermuda). In: Walter, M.R. (ed.). Stromatolites. Amsterdam, Elsevier, 381-388.

Ginsburg, R.N., 1960. Ancient analogues of recent stromatolites. 21st International Geological Congress, 22, 26-35.

Gónzalez, A., Pérez, A., 2018. El Terciario del sector turolense de la cuenca del Ebro: una crónica de la estructuración alpina de la Cordillera Ibérica. In: Alcalá, L., Calvo, P., Simón, J.L. (eds.). Geología de Teruel. Alcañiz, Instituto de Estudios Turolenses de la Diputación de Teruel, 83-98.

Gradziński, M., 2010. Factors controlling growth of modern tufa: results of a field experiment. In: Pedley, M., Rogerson, M. (eds.). Tufas and Speleothems: Unravelling the Microbial

and Physical Controls. London, The Geological Society, 336 (Special Publications), 143-191. DOI: https://doi.org/10.1144/SP336.8

Grotzinger, J.P., Knoll, A.H., 1999. Stromatolites in Precambrian carbonates: Evolutionary Mileposts or Environmental Dipsticks? Annual Review of Earth and Planetary Science, 27, 313-358. DOI: https://doi.org/10.1146/annurev.earth.27.1.313

Haq, B.U., 2014. Cretaceous eustasy revisited. Global and Planetary Change, 113, 44-58. DOI: https://doi.org/10.1016/j.gloplacha.2013.12.007

Hiatt, E.E., Pufahl, P.K., 2014, Cathodoluminescence petrography of carbonate rocks: application to understanding diagenesis, reservoir quality, and pore system evolution. In: Coulson, I. (ed.). Cathodoluminescence and its application to geoscience: Mineralogical Association of Canada. Short Course Series, 45, 75-96.

Hladil, J., Ruzicka, M., Koptikova, L., 2006. Stromatactis cavities in sediments and the role of coarse-grained accessories. Bulletin of Geosciences, 81(2), 123-146.

Hladil, J., Ruzicka, M., Geurts, B.J., Clercx, H., Uijttewaal, W., 2007. Stromatactic patterns formation in geological sediments: field observations versus experiments. Ercoftac Series, 11, 85.

Hoefs, J., 2009. Stable Isotope Geochemistry. Berlin, Springer-Verlag, 285pp.

Hofmann, H.J., 1973. Stromatolites: Characteristics and Utility. Earth-Science Reviews, 9, 339-373. DOI: https://doi.org/10.1016/0012-8252(73)90002-0

Huerta, P., Armenteros, I., Silva, P.G., 2011. Large-scale architecture in non-marine basins: the response to the interplay between accommodation space and sediment supply. Sedimentology, 58(7), 1716-1736. DOI: https://doi.org/10.1111/j.1365-3091.2011.01231.x

Ikejiri, T., Lu, Y., Zhang, B., 2020. Two-step extinction of Late Cretaceous marine vertebrates in northern Gulf of Mexico prolonged biodiversity loss prior to the Chicxulub impact. Scientific Reports, 10(1), 4169. DOI: https://doi.org/10.1038/s41598-020-61089-w

Isasmendi, E., Torices, A., Canudo, J.I., Currie, P.J., Pereda□Suberbiola, X., 2022. Upper Cretaceous European theropod palaeobiodiversity, palaeobiogeography and the intra□Maastrichtian faunal turnover: new contributions from the Iberian fossil site of Laño. Papers in Palaeontology, 8(1), e1419. DOI: https://doi.org/10.1002/spp2.1419

Jahnert, R.J., Collins, L.B., 2011. Significance of subtidal microbial deposits in Shark Bay, Australia. Marine Geology, 286, 106-111. DOI: https://doi.org/10.1016/j.margeo.2011.05.006

Jahnert, R.J., Collins, L.B., 2013. Controls on microbial activity and tidal flat evolution in Shark Bay, Western Australia. Sedimentology, 60, 1071-1099. DOI: https://doi.org/10.1111/sed.12023

Kano, A., Hagiwara, R., Kawai, T., Hori, M., Matsuoka, J., 2007. Climatic conditions and hydrological change recorded in a high-resolution stable-isotope profile of a recent laminated tufa on a subtropical island, southern Japan. Journal of Sedimentary Research, 77, 59-67. DOI: https://doi.org/10.2110/jsr.2007.006

Kennard, J.M., Burne, R.V., 1989. Stromatolite Newsletter Number 14. Camberra, Bureau of Mineral Resources, Geology and Geophysics, 179pp.

Le Loeuff, J., Buffetaut, E., Martin, M., 1994. The last stages of dinosaur faunal history in Europe: a succession of Maastrichtian dinosaur assemblages from the Corbières (southern France). Geological Magazine, 131(5), 625-630. DOI: https://doi.org/10.1017/S0016756800012413

Leng, M.J., Marshall, J.D., 2004. Palaeoclimate interpretation of stable isotope data from lake sediment archives. Quaternary Science Reviews, 23, 811-831. DOI: https://doi.org/10.1016/j.quascirev.2003.06.012

Liesa, C.L., Casas, A.M., Simón, J.L., 2018. La tectónica de inversión en una región intraplaca: La Cordillera Ibérica. Revista de la Sociedad Geológica de España, 31, 23-50.

Logan, B.W., Rezak, R., Ginsburg, R.N., 1964. Classification and environmental significance of algal stromatolites. The Journal of Geology, 72, 68-83. DOI: https://www.jstor.org/stable/30071097

Long, D.G., 2017. Evidence of flash floods in Precambrian gravel dominated ephemeral river deposits. Sedimentary Geology, 347, 53-66. DOI: https://doi.org/10.1016/j.sedgeo.2016.11.006

Machel, H.G., Burton, E., 1991. Factors governing cathodoluminescence in calcite and dolomite and their implications for studies of carbonate diagenesis. In: Barker, C.E., Kopp, O.C. (eds.). Luminescence Microscopy and Spectroscopy: Qualitative and Quantitative Applications. Society for Sedimentary Geology (SEPM) Short Course, 25, 37-58.

Martín-Bello, L., Arenas Abad, C., Alonso-Zarza, A.M., 2017. Preliminary interpretation of the stable-isotope composition in lacustrine stromatolites of the Sierra de Alcubierre (Miocene, Ebro Basin, Spain). Geogaceta, 61, 171-174.

Martín□Bello, L., Arenas, C., Jones, B., 2019. Lacustrine stromatolites: Useful structures for environmental interpretation–an example from the Miocene Ebro Basin. Sedimentology, 66(6), 2098-2133. DOI: https://doi.org/10.1111/sed.12577

Martín-Chivelet, J., Giménez, R., 1992. Palaeosols inmicrotidal carbonate sequences, Sierra de Utiel Formation, Upper Cretaceous, SE Spain. Sedimentary Geology, 81, 125-145. DOI: https://doi.org/10.1016/0037-0738(92)90060-5

Martín-Chivelet, J., Floquet, M., García-Senz, J., Callapez, P.M., López-Mir, B., Muñoz, J.A., Dinis, P.M., 2019. Late Cretaceous post-rift to convergence in Iberia. In: Quesada, C., Oliveira, J.T. (eds.). The Geology of Iberia: A Geodynamic Approach. Heidelberg, Springer, 285-376.

McGowan, J.H., Groat, G.C., 1971. Van Horn Sandstone, West Texas: an alluvial fan model for mineral exploration. Bureau of Economic Geology, University of Texas, 72, 57pp.

McKenzie, J.A., 1985. Stable-isotope mapping in Messinian evaporative carbonates of central Sicily. Geology, 13(12), 851-854. DOI: https://doi.org/10.1130/0091-7613(1985)13%3C851:SMIMEC%3E2.0.CO;2

Mercedes-Martín, R., Salas, R., Arenas, C., 2014. Microbial-dominated carbonate platforms during the Ladinian rifting: Sequence stratigraphy and evolution of accommodation in a fault-controlled setting (Catalan Coastal Ranges, NE Spain). Basin Research, 26, 269-296. DOI: https://doi.org/10.1111/bre.12026

Meyers, W.J., 1978. Carbonate cements: their regional distribution and interpretation in Mississippian lime- stones of southwestern New Mexico. Sedimentology, 25, 371-400. DOI: https://doi.org/10.1111/j.1365-3091.1978.tb00318.x

Miall, A.D., 1977. A review of the braided-river depositional environment. Earth-Science Reviews, 13(1), 1-62. DOI: https://doi.org/10.1016/0012-8252(77)90055-1

Monty, C.L.V., 1976. The origin and development of cryptalgal fabrics. In: Walter, M.R. (ed.). Stromatolites, Developments in Sedimentology, 20, 193-249. DOI: https://doi.org/10.1016/S0070-4571(08)71137-3

Monty, C.L., Mas, J.R., 1981. Lower Cretaceous (Wealdian) blue-green algal deposits of the province of Valencia, eastern Spain. In: Monty, C. (ed.). Phanerozoic stromatolites: case histories. Berlin, Heidelberg, Springer, 85-120.

Nichols, G.J., Fisher, J.A., 2007. Processes, facies and architecture of fluvial distributary system deposits. Sedimentary Geology, 195(1-2), 75-90. DOI: https://doi.org/10.1016/j.sedgeo.2006.07.004

Nickel, E., 1983. Environmental significance of freshwater oncoids, Eocene guarga formation, Southern Pyrenees, Spain. In: Peryt, T.M. (ed). Coated grains. Berlin, Heidelberg, Springer, 308-329.

Noffke, N., Awramik, S.M., 2013. Stromatolites and MISS — Differences between relatives. Geological Society of America (GSA) Today, 23, 4-9.

Ordóñez, S., García del Cura, M., 1977. Facies oncolíticas en medio continental: Aplicación al sector SE de la Cuenca del Duero. Estudios geológicos, 33, 459-466.

Ordóñez, S., García del Cura, M., 1983. Recent and Tertiary fluvial carbonates in Central Spain. Modern and ancient fluvial systems, 485-497. DOI: https://doi.org/10.1002/9781444303773.ch39

Ordóñez, S., Carballal, R., García del Cura, A., 1980. Carbonatos biogénicos actuales en la cuenca del río Dulce (provincia de Guadalajara). Boletín de la Real Sociedad Española de Historia Natural (Sección Geológica), 78, 303-315.

Ordóñez, S., Martín, J.G., Del Cura, M.G., Pedley, H.M., 2005. Temperate and semi-arid tufas in the Pleistocene to Recent fluvial barrage system in the Mediterranean area: The Ruidera Lakes Natural Park (Central Spain). Geomorphology, 69(1-4), 332-350. DOI: https://doi.org/10.1016/j.geomorph.2005.02.002

Parcerisa, D., Gómez-Gras, D., Martín-Martín, J.D., 2006. Calcretes, oncolites, and lacustrine limestones in Upper Oligocene alluvial fans of the Montgat area (Catalan Coastal Ranges, Spain). In: Alonso-Zarza, A.M., Tanner, L.H. (eds.). Paleoenvironmental Record and Applications of Calcretes and Palustrine Carbonates. London, Geological Society of America, 416, 105-117. DOI: https://doi.org/10.1130/2006.2416(07)

Pérez, A., Pardo, G., Villena, J., González, A., 1983. Estratigrafía y sedimentología del Paléogeno de la cubeta de Montalbán, prov. de Teruel, España. Boletín de la Real Sociedad Española de Historia Natural, Sección Geológica, 81(3-4), 197-223.

Petryshyn, V.A., Corsetti, F.A., Berelson, W.M., Beaumont, W., Lund, S.P., 2012. Stromatolite lamination frequency, Walker Lake, Nevada: Implications for stromatolites as biosignatures. Geology, 40, 499-502. DOI: https://doi.org/10.1130/G32675.1

Platt, N.H., 1989. Lacustrine carbonates and pedogenesis: sedimentology and origin of palustrine deposits from the Early Cretaceous Rupelo Formation, W Cameros Basin, N Spain. Sedimentology, 36, 665-684. DOI: https://doi.org/10.1111/j.1365-3091.1989.tb02092.x

Platt, N.H., Wright, V.P., 1991. Lacustrine carbonates: facies models, facies distributions and hydrocarbon aspects. In: Anadón, P., Cabrera, L., Kelts, K. (eds.). Lacustrine Facies Analysis. Special Publication International Association of Sedimentologists, 13, 57-74. DOI: https://doi.org/10.1002/9781444303919.ch3

Plaziat, J.C., 1984. Le domaine Pyrénnéen de la fin du Crétacé à la fin de l'Éocène. Stratigraphie, paléoenvironnements et évolution paléogéographique. PhD Thesis. Orsay, Université Paris-Sud, 1362pp.

Prieto-Márquez, A., Dalla Vecchia, F.M., Gaete, R., Galobart, À., 2013. Diversity, relationships, and biogeography of the lambeosaurine dinosaurs from the European Archipelago, with description of the new aralosaurin Canardia garonnensis. PLoS One, 8(7), e69835. DOI: https://doi.org/10.1371/journal.pone.0069835

Renaut, R.W., Owen, R.B., Jones, B., Tiercelin, J.J., Tarits, C., Ego, J.K., Konhauser, K.O., 2013. Impact of lake-level changes on the formation of thermogene travertine in continental rifts: Evidence from Lake Bogoria, Kenya Rift Valley. Sedimentology, 60, 428-468. DOI: https://doi.org/10.1111/j.1365-3091.2012.01347.x

Riding, R., 1991. Classification of microbial carbonates. In: Riding, R. (ed.). Calcareous Algae and Stromatolites. Berlin, Springer-Verlag, 21-51. DOI: https://doi.org/10.1007/978-3-642-52335-9_2

Riding, R., 2000. Microbial carbonates: The geological record of calcified bacterial-algal mats and biofilms. Sedimentology, 47, 179-214. DOI: https://doi.org/10.1046/j.1365-3091.2000.00003.x

Riding, R., 2008. Abiogenic, microbial and hybrid authigenic carbonate crusts: components of Precambrian stromatolites. Geologica Croatica, 61(2-3), 73-103. DOI: https://doi.org/10.4154/GC.2008.10

Riding, R., 2011. Microbialites, stromatolites and thrombolites. In: Reitner, J., Thiel, V. (eds.). Encyclopedia of Geobiology. Heidelberg, Springer, 635-654. DOI: https://doi.org/10.1007/978-1-4020-9212-1_196

Roche, A., Vennin, E., Bouton, A., Olivier, N., Wattinne, A., Bundeleva, I., Deconinck, J.F., Virgone, A., Gaucher, E.C.,

Visscher, P.T., 2018. Oligo-Miocene lacustrine microbial and metazoan buildups from the Limagne Basin (French Massif Central). Palaeogeography, Palaeoclimatology, Palaeoecology, 504, 34-59. DOI: https://doi.org/10.1016/j.palaeo.2018.05.001

Salas, R., Casas, A., 1993. Mesozoic extensional tectonics, stratigraphy, and crustal evolution during the Alpine cycle of the eastern Iberian Basin. Tectonophysics, 228, 33-55. DOI: https://doi.org/10.1016/0040-1951(93)90213-4

Salas, R., Guimerà, J., Mas, R., Martín-Closas, C., Meléndez, A., Alonso, A., 2001. Evolution of the Mesozoic Central Iberian Rift System and its Cainozoic inversion (Iberian Chain). In: Ziegler, P.A., Cavazza, W., Robertson, A.H.F., Crasquin-Soleau, S. (eds.). Peri-Tethys Memoir 6: Peri-Tethyan Rift/Wrench Basins and Passive Margins. Paris, Mémoires du Muséum National d'Histoire Naturelle, 186,145-186.

Sánchez-Moya, Y., Sopeña, A., 2004. El Rift Mesozoico Ibérico. In: Vera, J.A. (ed.). Geología de España. Madrid, Sociedad Geológica de España and Instituto Geológico y Minero de España, 484-522.

Sanz, M.E., Alonso-Zarza, A.M., Calvo, J.P., 1995. Carbonate pond deposits related to semi-arid alluvial systems: examples from the Tertiary Madrid Basin, Spain. Sedimentology, 42, 437-452. DOI: https://doi.org/10.1111/j.1365-3091.1995.tb00383.x

Segura, M., García Hidalgo, J.F., Carenas, B., Gil, J., García, A., 2004. Evolución paleogeográfica de la Cuenca Ibérica en el Cretácico Superior. Geogaceta, 36, 103-116.

Sellés, A.G., Vila, B., 2015. Re-evaluation of the age of some dinosaur localities from the southern Pyrenees by means of megaloolithid oospecies. Journal of Iberian Geology, 41(1), 125-139. DOI: https://doi.org/10.5209/rev_JIGE.2015.v41.n1.48659

Seong-Joo, L., Browne, K.M., Golubic, S., 2000. On stromatolite lamination. In: Riding, R., Awramik, S.M. (eds.). Microbial Sediments. Berlin, Springer-Verlag, 16-24. DOI: https://doi.org/10.1007/978-3-662-04036-2_3

Sequero, C., Aurell, M., Bádenas, B., 2020. Oncoid distribution in the shallow domains of a Kimmeridgian carbonate ramp (Late Jurassic, NE Spain). Sedimentary Geology, 398, 105585. DOI: https://doi.org/10.1016/j.sedgeo.2019.105585

Shapiro, R.S., Fricke, H.C., Fox, K., 2009. Dinosaur-bearing oncoids from ephemeral lakes of the Lower Cretaceous Cedar Mountain Formation, Utah. Palaios, 24(1), 51-58. DOI: https://doi.org/10.2110/palo.2008.p08-013r

Sheehan, P.M., Harris, M.T., 2004. Microbialite resurgence after the Late Ordovician extinction. Nature, 430(6995), 75-78. DOI: https://doi.org/10.1038/nature02654

Sohn, Y.K., Rhee, C.W., Kim, B.C., 1999. Debris flow and hyperconcentrated flood-flow deposits in an alluvial fan, northwestern part of the Cretaceous Yongdong Basin, Central Korea. The Journal of Geology, 107(1), 111-132. DOI: https://doi.org/10.1086/314334

Suarez-Gonzalez, P., Quijada, I.E., Benito, M.I., Mas, R., Merinero, R., Riding, R., 2014. Origin and significance of lamination in Lower Cretaceous stromatolites and proposal for a quantitative approach. Sedimentary Geology, 300, 11-27. DOI: https://doi.org/10.1016/j.sedgeo.2013.11.003.

Teranes, J.L., McKenzie J.A., 2001. Lacustrine oxygen isotope record of 20th-century climate change in central Europe: Evaluation of climatic controls on oxygen isotopes in precipitation. Journal of Paleolimnology, 26, 131-146. DOI: https://doi.org/10.1023/A:1011175701502

Torromé, D., Aurell, M., 2024. Upper Campanian continental oncolites in the Montalbán subbasin (Allueva Fm., Iberian Chain). Geogaceta 75, 3-6.

Torromé, D., Aurell, M., Bádenas, B., 2022. A mud-dominated coastal plain to lagoon with emerged carbonate mudbanks: the imprint of low-amplitude sea level cycles (mid-Upper cretaceous, South Iberian Ramp). Sedimentary Geology, 476, 106178. DOI: https://doi.org/10.1016/j.sedgeo.2022.106178

Torromé, D., Aurell, M., Martín-Pérez, A., Košir, A., 2023. A carbonate palustrine system with marshes and shallow ephemeral lakes (Campanian, northeastern Iberian Basin). Sedimentary Geology, 456, 106516. DOI: https://doi.org/10.1016/j.sedgeo.2023.106516

Vázquez-Urbez, M., Arenas, C., Sancho, C., Osácar, C., Auqué, L., Pardo, G., 2010. Factors controlling present day tufa dynamics in the Monasterio de Piedra Natural Park (Iberian Range, Spain): depositional environmental settings, sedimentation rates and hydrochemistry. International Journal of Earth Sciences, 99, 1027-1049. DOI: https://doi.org/10.1007/s00531-009-0444-2

Vázquez-Urbez, M., Arenas, C., Pardo, G., Pérez- Rivarés, J., 2013. The effect of drainage reorganization and climate on the sedimentologic evolution of intermontane lake systems: the final fill stage of the Tertiary Ebro Basin (Spain). Journal of Sedimentary Research, 83, 562-590. DOI: https://doi.org/10.2110/jsr.2013.47

Vicente, A., Expósito, M., Sanjuan, J., Martín-Closas, C., 2016. Small sized charophyte gyrogonites in the Maastrichtian of Coll de Nargó, Eastern Pyrenees: An adaptation to temporary floodplain ponds. Cretaceous Research, 57, 443-456. DOI: https://doi.org/10.1016/j.cretres.2015.07.017

Vila, B., Sellés, A.G., Brusatte, S.L., 2016. Diversity and faunal changes in the latest Cretaceous dinosaur communities of southwestern Europe. Cretaceous Research, 57, 552-564. DOI: https://doi.org/10.1016/j.cretres.2015.07.003

Woo, K.S., Khim, B.K., Yoon, H.S., Lee, K.C., 2004. Cretaceous lacustrine stromatolites in the Gyeongsang Basin (Korea): records of cyclic change in paleohydrological condition. Geosciences Journal, 8, 179-184. DOI: https://doi.org/10.1007/BF02910193

Zamarreño, I., Anadón, P., Utrilla, R., 1997. Sedimentology and isotopic composition of Upper Palaeocene to Eocene non-marine stromatolites, eastern Ebro Basin, NE Spain. Sedimentology, 44, 159-176. DOI: https://doi.org/10.1111/j.1365-3091.1997.tb00430.x

Manuscript received May 2024;
revision accepted October 2024;
published Online December 2024.